

Performance of McRAS-AC in the GEOS-5 AGCM: Part 1, Aerosol-
activated Cloud Microphysics, Precipitation, Radiative Effects, and
Circulation

Y.C. Sud¹, D. Lee^{1,2,3}, L. Oreopoulos¹, D. Barahona¹⁴, A. Nenes⁵, and M. J. Suarez¹

[1] {NASA Goddard Space Flight Center, Greenbelt, MD, USA}

[2] {University Space Research Association, Columbia, MD, USA}

[3] {Seoul National University, Seoul, South Korea}

[4] {I.M. Systems Group Inc., Rockville, Maryland, USA}

[5] {School of Atmospheric and Earth Science, Georgia Tech. Atlanta, Georgia, USA}

Correspondence to: Y.C.Sud (yogesh.c.sud@nasa.gov)

Abstract

A revised version of the Microphysics of clouds with Relaxed Arakawa-Schubert and Aerosol-Cloud interaction (McRAS-AC), including, among others, the Barahona and Nenes ice nucleation parameterization, is implemented in the GEOS-5 AGCM. Various fields from a 10-year long integration of the AGCM with McRAS-AC were compared with their counterparts from an integration of the baseline GEOS-5 AGCM, and with satellite data as observations. Generally using McRAS-AC reduced biases in cloud fields and cloud radiative effects are much better over most of the regions of the Earth. Two weaknesses are identified in the McRAS-AC runs, namely, too few cloud particles around 40S-60S, and too high cloud water path during northern hemisphere summer over the Gulf Stream and North Pacific. Sensitivity analyses showed that these biases potentially originated from biases in the aerosol input. The first bias is largely eliminated in a sensitivity test using 50% smaller aerosol particles, while the second bias is much reduced when interactive aerosol chemistry was turned on. The main drawback of McRAS-AC is dearth of low-level marine stratus clouds, probably due to lack of dry-convection, not yet implemented into the cloud scheme. Despite these biases, McRAS-AC does simulate realistic clouds and their optical properties that can improve with better aerosol-input and thereby has the potential to be a valuable tool for climate modeling research because of its aerosol indirect effect simulation capabilities involving prediction of cloud particle number concentration and effective particle size for both convective and stratiform clouds is quite realistic.

1 Introduction

Traditionally, meteorologists focused on severe weather and precipitation forecasts. Not much attention was paid to cloud water. There are two reasons for this. First, in-cloud water is generally less than 5% of precipitation generated in a typical weather episode; second, weather forecast is useful for a week or less, and on that time-span, cloudiness and its radiative effects on the synoptic weather systems are small. Consequently, *ad hoc* ways to assess cloud radiative forcing were deemed sufficient. However, once the emphasis of forecasting turned to climate, radiative forcing and everything that affects it including influence of aerosols on clouds, cloud radiative effects (CRE), and greenhouse gases become very important. Among them, cloud-aerosol interaction (Andreae and Rosenfeld, 2008) is in

early stages of development (e.g., Quaas et al., 2003, Roelofs et al., 2006, Sud and Lee, 2007; Morrison, and Gettelman 2008, Liu et al., 2011). Our paper deals with evaluating a recently revised and updated aerosol-cloud interaction (AC) module of an established cloud scheme called McRAS (Microphysics of clouds with Relaxed Arakawa-Schubert convection) that is implemented in the GEOS-5 AGCM for evaluating its performance.

The pioneering works of Gibbs (1876, 1878), and Köhler (1936) laid the foundation of the physics of aerosol-activation from first principles of thermodynamics. Recent developments of physically based aerosol activation parameterizations are due to Abdul-Razzak and Ghan (2000, 2002), Nenes et al. (2001), Nenes and Seinfeld, (2003), Liu and Penner (2005) and Barahona and Nenes (2009). More aerosols generally increase the number density of cloud particles (CP) (Twomey, 1979; Seinfeld and Pandis, 1996) and thereby suppress autoconversion and accretion that form precipitating hydrometeors (e.g., Albercht, 1989; Seifert and Beheng, 2001, 2005). We cite a few recent studies that show the impact of aerosols on i) weather and climate prediction (Krishnamurti *et al.*, 2009; Sud *et al.*, 2009; Wilcox *et al.*, 2009) with GEOS-4 AGCM; ii) the diurnal and seasonal cycles of precipitation (Kim et al., 2010); iii) the weekly cycle of precipitation over central North America (Bell et al., 2009b); iv) increase in the incidence of tornados (e.g., Rosenfeld and Bell, 2011) and lightening (Bell et al, 2009a), v) the vertical stability of the atmosphere leading to an elevated heat pump hypothesis affecting the Indian monsoons (Lau and Kim, 2007), and vi) freezing of in-cloud drops with release of latent heat of freezing (Rosenfeld et al., 2000, 2006). The debate on how and/or how much do aerosols influence different clouds to foster or suppress precipitation yield from different cloud types continues (e.g., Koren et al., 2012; Gunturu, 2010, and Li et al., 2011). An outcome of increasing cloud particle number concentrations (CPNC) is the accompanying reduction in cloud particle sizes in the distribution. It slows the auto-conversion and accretion of cloud drops to form precipitation size hydrometeors and that gives liquid cloud particles and embryonic raindrops the time to ascend in the convective updrafts and glaciate at subfreezing temperatures to latent heat of freezing and further boost the updraft buoyancy. How this plays out in the real world under a variety of convective scenarios, depends upon how much further the convective towers ascend and how much additional condensate and precipitation is generated.

Numerical models can simulate all of the above features, if the cloud-physics processes are realistically parameterized and the ambient atmosphere has realistic aerosols. However,

1 many GCMs still obtain clouds invoking a number of simplifying and/or *ad hoc* assumptions
2 (Bougeault and Geleyn, 1996; Randall 2010) that often ignore the aerosol effects on clouds.
3 At the present time, even understanding of the climatic impact of aerosols remains uncertain
4 (IPCC 2007), while modelers endeavor to include them in their cloud schemes and
5 intercompare their performance with other models (Bellouin et al., 2011). Without realistic
6 aerosol input, simulated CPNC consisting of liquid and ice cloud particle number
7 concentrations (hereafter LPNC, IPNC), also get affected and real benefits of including
8 aerosol-cloud interaction become uncertain. A notable inference of cloud seeding
9 experiments, as summarized by Cotton and Pielke (1995), is that with a limited window of
10 opportunity, cloud seeding becomes a hit or miss venture and its full potential is not realized.
11 One easily infers that to observationally verify the impact, the atmospheric aerosols too must
12 be known reasonably well at the scales of clouds.

13 Aside from CPNC enhancement via shattering and splintering of the already existing
14 cloud particles aerosol activation for liquid particles or ice nucleation for cloud ice particles is
15 the only source of new CPs. A well designed aerosol-cloud-radiation interaction model, such
16 as McRAS, can therefore provide a better physical basis for determining the benefits of
17 interactive aerosols in a cloud scheme. McRAS was renamed as McRAS-AC after the aerosol
18 cloud interaction was included. The question we want to address is whether McRAS-AC is a
19 worthwhile option to simulate the cloud optical properties and climate in the GEOS-5 GCM?

20 Some issues with simulating mixed phase clouds are proverbial. The major one is getting
21 mixed phase water and ice mass fractions, effective sizes, and apportionment of precipitation
22 in to liquid and ice particles. Based on the vertical velocity and entrainment rate, IN nucleate
23 cloud ice particles. In addition we perform mass transfer from liquid to ice particles by
24 Bergeron-Findeisen process in the following manner. At subfreezing temperatures, the vapor
25 pressure differences over cloud water and ice particles are large enough to produce a
26 substantial vapor pressure gradient between them to induce mass transfer of cloud water-to-
27 cloud ice through the intervening atmosphere. Simultaneously, precipitating hydrometeors
28 collect cloud water/ice particles during fall through a cloud (even from clear air that happens
29 to be supersaturated with respect to the ice). In this way, precipitation removes cloud particle-
30 mass and reduces the in-cloud CPNC. Altogether, these processes add up to make the sink
31 term of CPs for which each of the components must be parameterized. The sum of source and
32 sink terms yields the time rate of change of mass and number concentration as shown in

Morrison and Gettelman (2008). To close the system, one also needs a precipitation microphysics scheme. Thus an end-to-end aerosol-cloud interaction parameterization starts with aerosols activating as CCN and/or IN nucleating ice to receive condensation and/or ice deposition; needs a reasonable treatment of mass transfers among liquid, ice and vapor phases of cloud water with precipitation microphysics for liquid and ice clouds. Most present-day GCM modelers have started to include prognostic parameterizations of the direct and indirect aerosol effects in the cloud schemes, but several complexities and uncertainties still confound them. For example, aerosol input, implying their size distribution and speciation and their hygroscopic properties, and activation/nucleation potential for CCN/IN, which must be inferred from aerosol chemistry, are themselves uncertain and are going through extensive validation and upgrading tests. The ultimate challenge is to make the aerosol-cloud-radiation scheme realistic enough to affect the key aspects of cloud-radiative interactions realistic enough to better simulate the climate, and respond to aerosol direct and indirect effects. Section 2 gives a brief description of GEOS-5 AGCM hosting McRAS-AC as one of its options. Section 3 gives the simulation experiments. Section 4 gives simulation results and key biases. Section 5 has summary and conclusions and research directions to make MCRAS-AC simulations more realistic.

2 Cloud Schemes: GEOS-5 GCM and McRAS-AC

2.1 GEOS-5 GCM

The Fortuna 2.5 version of the GEOS-5 GCM is documented by Molod et al. (2012); it describes the model performance with several new updates to the earlier MERRA version (Rinecker et al., 2008). Briefly, it employs Relaxed Arakawa-Schubert scheme (RAS) due to Moorthi and Suarez (1992) for moist convection with PDFs of cloud water for cloud microphysics. RAS produces prognostic cloud-cover, and diagnostic ice mixing ratios, and cloud water. Other upgrades comprise of large-scale condensation and evaporation, auto-conversion and accretion of cloud water and ice, sedimentation of cloud-ice, and re-evaporation of falling precipitation following Bacmeister et al. (2006). Its long-wave radiative transfer calculations are due to Chou and Suarez (1994), and its shortwave radiative transfers are due to Chou (1998, 1999). These handle interactions with simulated clouds, cloud water, water vapor, and externally prescribed trace gases. In addition, shortwave calculation includes absorption, scattering and transmission by aerosols, i.e., it treats the direct effect of aerosols

only. For full details, refer to Molod et al. (2012) and Rinecker et al. (2008). We will refer to the AGCM as baseline GEOS-5 AGCM.

2.2 McRAS-AC

The latest version of McRAS (Sud and Walker, 2003a) is chosen as the cloud scheme for including the aerosol-cloud interactions. Its evolution dates back to development and evaluation of McRAS built from RAS moist convection. McRAS uses cloud microphysics based on the work of Sundqvist (1988) and Tiedtke (1993) along with other upgrades namely rain-evaporation (Sud and Molod, 1988) and convective downdrafts (Sud and Walker, 1993). It is extensively evaluated in a Single Column Model (Sud and Walker, 1999a, Ghan et al., 2000, Xie et al., 2002). Its climate simulations with GEOS-2 GCM (Sud and Walker, 1999b) are more realistic than that of the baseline mode used. It produced reasonable intra-seasonal oscillations (ISO) in GEOS-2 and GEOS-3 AGCMs. The ISOs were well reproduced even in the NCAR implementation (Maloney and Hartmann, 2000). Nevertheless, these GCM applications also highlighted some weaknesses that were addressed in subsequent upgrades (Sud and Walker, 2003a,b). Without aerosol-cloud interaction to provide LPNC or ICNC, McRAS used empirical equations by Sundqvist (1988) for estimating precipitation production rate as a function of cloud water, ambient temperature, and cloud type. For radiation, in-cloud CPNC were assumed for land and ocean following Del Genio et al. (1996), while the volume and effective radii of CPs were estimated from another set of empirical assumptions (Sud and Walker, 1999a).

The current aerosol-cloud interaction microphysics modules are documented in Sud and Lee (2007). The new option is the use of Barahona and Nenes (2009a) as an alternative to Liu and Penner (2005) aerosol nucleation for IN. The version of McRAS-AC used herein has McRAS cloud-scheme plus Fountoukis and Nenes (2005) aerosol activation parameterization to yield CCN and Barahona and Nenes (2009a) scheme for ice nucleation to yield IN and Sud and Lee (2007) precipitation microphysics for liquid and Sundqvist (1988) for precipitation emerging from mixed phase and ice clouds. Together, these are the sources of LPNC and IPNC for water and ice clouds, respectively. In-cloud evaporation and/or precipitation and self collection of cloud water are parameterized by Sud and Lee (2007), which is a recast of Seifert and Beheng (2001) to obtain relations for thicker clouds encountered in a coarse resolution GCM. Any change in cloud mass by condensation/deposition and subsequent removal by precipitation, works interactively through an implicit backward numerical

solution that is an approximation for the nonlinear coupled differential equations that are impossible to solve without iteration. Lacking an IPCN based snow precipitation scheme, McRAS-AC currently uses Sundqvist (1988) parameterization for mixed phase and ice phase precipitation. However, inclusion of ice nucleation (IN) (Barahona and Nenes, 2009a,b) and Bergeron-Findeisen cloud water-to-ice mass transfer (Rotstayn, 2000) cloud liquid and ice mass fractions and corresponding CPNC (LPNC plus IPNC) are calculated consistently to conserve mass and IPNC budgets. Nevertheless, CPNC reduction is non-linear and is based on a curve-fitted relationship between cloud mass and number concentration for an assumed Gamma distribution of cloud particle sizes. Homogenous freezing of in-cloud water drops surviving until -38°C is enforced through instantaneous freezing of LPNC into IPNC. The above processes, carried out by several modules, provide an end-to-end treatment of prognostic cloud water mass (apportioned between liquid and ice) and CPNC, and precipitation into liquid and snow hydrometeors. Its present implementation is shown through a block diagram, Figure 1. It shows how aerosol activation by vertical ascent or its equivalent cooling creates condensate while Sud and Lee (2007) and Sundqvist (1988) cloud micro physics create precipitation and reduce the CPNC. McRAS-AC is implemented as an option to work with the baseline GEOS-5 GCM. For more details, the reader may like to refer to the original papers referenced above.

3. Simulation Experiments

We performed two 10-year long simulations, one with the baseline Fortuna 2.5 version of the GEOS-5 AGCM (referred to as baseline) with its own cloud scheme and one with the same GEOS-5 AGCM, but for the newly implemented McRAS-AC cloud physics module as an option in the AGCM (See details in Table 1 for differences). There are two more differences: one in the use of simulated clouds without any scaling of cloud fraction, and one is use of GEOS-5 AGCM PBL cloud treatment instead of the dry convection based in McRAS-AC. The dry eddy transports pulls up the near surface water vapor to the level of neutral buoyancy near the PBL top, whereby it raises the height of the cloud base and dries the boundary layer. In the present implementation, McRAS-AC relies on the PBL scheme of the baseline model. The monthly climatologies of aerosols are taken from GOCART (Chin et al, 2002) and are based on extensive aerosol model development and calibration/validation exercises at GSFC (Colarco et al., 2010). Currently we use five externally mixed aerosols namely sulfates, sea-

1 salt, mineral dust, black carbon and organic carbon. GOCART model generates time-series of
2 mass balances of different aerosol species. The aerosol numbers are calculated by making
3 sectional of aerosol sizes, called modes. The present goal is to determine if McRAS-AC can
4 perform reasonably well in the GEOS-5 AGCM and qualify to perform studies of the
5 influence of aerosols on cloud microphysics and cloud radiative effects (CRE).

7 **4. Results**

8 A comparison of two 10 year integrations, one with McRAS-AC in the GEOS-5 AGCM
9 (hereafter referred to as “MAC”) and one with the baseline GEOS-5 AGCM (hereafter,
10 referred to as “CTL”) examine precipitation, clouds, their water paths, and effective radii, and
11 CREs. There are two aspects of this intercomparison; one is the differences due to cloud
12 parameterization schemes in CTL and MAC, the other is the influence of aerosol activation
13 and associated cloud particle numbers and sizes; however, the effective radii of cloud liquid
14 and ice particles are empirically prescribed in CTL runs as functions of temperature and
15 cloud water path. The two most intractable component of the simulated climate change are the
16 CREs and how these would change with any climate change scenario. GCMs need to simulate
17 realistic (implying bias free) CREs. The goal here is to determine how MAC and CTL
18 climatologies compare with each other and how well they hold up against observations. Can
19 they simulate the annual cycle reasonably well, and, how much can we trust the model to
20 produce realistic CRE changes in simulating a climate change scenario of the future?
21 Specifically the aim is to evaluate MAC seasonal climatology biases and thereafter design
22 upgrades to ameliorate them. Second, are there reasonable sensitivities to aerosol mass and
23 number concentration of the real environment, and can they be used to improve model
24 model’s CREs and understand the influence of aerosols on clouds, and cloud-radiation
25 interactions and its consequences on the regional climate change? We produced MAC and
26 CTL seasonal average fields for DJF, MAM, JJA, SON and an annual mean for several key
27 fields. However, to keep figures-volume low, we only show the climatologies of the two
28 extreme seasons, DJF and JJA, and the annual means. Although revising the algorithms and
29 making aerosol input modifications to ameliorate some of the biases are left for Part 2 of the
30 paper; we will include two test runs that have potential to eliminate both biases of McRAS-
31 AC clouds identified herein. The following are the key highlights of our findings.

4.1 Precipitation Fields

The left two panels of Fig. 2 depict the broad feature of rainfall climatology of MAC and CTL. Both model-simulations have reasonable ITCZ and SPCZ, with intense convective rainfall, as expected. In DJF intense rainfall occurs over the South American landmass, Australia, the tropical islands of Southeast Asia follow the North Pacific Ocean currents, and the eastern seaboard of continental United States and the Gulf Stream. Large rainfall also occurs over the rising branch of Ferrell cell between 40S-60S. In JJA, we see tropical rain including the ITCZ at its northward location. The simulated tropical Pacific ITCZ is somewhat weaker with less than observed rainfall intensities in the mid-span of the Pacific ITCZ and somewhat stronger than observed near the land masses at both ends on land, presumably due to orographic intensification of precipitation; thus more water vapor converges on to land away from its natural location(s) over the ocean where the simulated rainfall climatology has a deficit. Indian and Asian regions have realistic monsoons and associated rainfall. Northwards of Sahel, the Sahara desert is dry in JJA as it should be. Generally, MAC and CTL biases in precipitation are quite similar to each other and hence the differences from observations are also similar. MAC does somewhat better on the RMSE scores in DJF and JJA but not on ANN (see Table 3). The majority of the biases are associated with orographic intensification of precipitation and its related moisture convergences, a proverbial problem with a number of numerical models that has been largely solved according to Chao (2012), but the Chao-code is not implemented in the Fortuna 2.5 version of GEOS-5 AGCM. In DJF one sees excessive rainfall biases along southern Andes, hilly regions of South Africa, and tropical islands of south East Asia. Precipitation biases around eastern regions of Himalayas, and Andes through South and Central America (red color in the difference maps). MAC or CTL simulation minus observations, the rainfall biases are more positive over the tropical Pacific ITCZ in CTL versus MAC whereas the biases are quite similar in the JJA over the tropical Pacific ITCZ except that lighter colors in MAC minus OBS means that the corresponding biases are lesser in MAC. Overall, both simulations, MAC and CTL, do reasonably well in comparison to GPCP precipitation data. In the boreal winter (DJF) season, MAC (CTL) simulate global mean precipitation of 2.89 (2.84) mm/day versus the somewhat smaller value of 2.68 mm/day in the GPCP data. The corresponding boreal summer (JJA) values are 3.01 (3.04) mm/day versus 2.71 mm/day in the GPCP data. Indeed, the simulated precipitation values are consistent with global mean surface evaporation. Accordingly, global condensation heating of McRAS-AC are 6.0 (8.7) Wm^{-2} in

DJF (JJA) larger. Since SSTs are prescribed, excessive evaporation over the oceans can occur without any negative feedback that could reduce the SSTs evaporation. (See Table 3 for the details of data).

DJF averages in the tropics show that the MAC (CTL) rainfall distribution over the sharp ITCZ is less (more) intense than the GPCP data. However, MAC simulations make up for the reduction with small increases over the grid cells north and south of the ITCZ. The orographic rainfall intensification biases are consistently positive and quite similar in both MAC and CTL simulations. Clearly, the GCM has a problem reproducing observed precipitation with flow across the steep hills; this is a persistent bias whose solution has remained elusive. For JJA, both MAC and CTL simulations the Equatorial Pacific ITCZ in the middle of its east-west span is weak similarly, even though CTL simulation has a slightly better organized ITCZ. On the whole, both cloud schemes show significant biases that need some attention.

In NH winter, precipitable water and precipitation yields are relatively small; accordingly, the magnitudes of DJF biases are also smaller compared to the warmer southern latitudes. Correspondingly, precipitation biases over the upslope regions of high orography are also smaller. McRAS-AC with all the extra degrees of freedom turned out to as realistic as the baseline GCM. In JJA, the CTL Indian monsoon rainfall is slightly better than MAC, but the structure of the biases is very similar, while the differences in the biases are relatively small. Thus comparing precipitation biases in MAC and CTL simulations, deficiencies of McRAS-AC in some regions despite its better CRE does not warrant keeping McRAS in the development phase of climate simulation studies in which CREa and precipitation changes are vital for understanding climate change.

Moreover, differences that are statistically significant are important. When this is done with each model simulation minus observations, the orographically enhanced precipitation biases overwhelmed the outcome, but when the analysis is done on rainfall differences between the two models runs, we isolate areas that show the influence of moist physics only (Figure 3). Large differences are notable over the tropical ITCZ that includes East Pacific in DJA and mid Pacific in JJA; some differences are significant over the tropical Atlantic and Indian Ocean in both seasons. In these convergence zones MAC precipitation is less than that of CTL. Naturally, areas of statistical significance on annual mean fields are even smaller in conformity with our understanding that biases often reduce by averaging not only the annual cycle but also across space and multi-model ensembles even over shorter time periods.

Overall, the rainfall differences between MAC and CTL in a 2-tailed student t-test at 95% significance are small and without much structure except for ice-covered Polar Regions. Thus both schemes produce similar rainfall fields with very similar biases vis-à-vis GPCP data barring the biases introduced by orographic intensification which really gives large biases with respect to GPCP data.

4.2 Cloud Fractions and Water Path

Cloud fractions and in-cloud water particle number concentration are two fields that govern the most important field, the CREs (Section 4.5.1); hence biases in cloud radiation fields of the shortwave and longwave radiation can be linked to the biases in cloud fraction and cloud water path and effective radius. The vertical alignment of clouds (Lazaros et al., 2012) or the prescribed cloud water-path also influences the CREs. These are discussed at length in the subsections of Section 4.5

4.2.1 Cloud fractions

We show yearly average zonal mean cloud fractions for the atmospheric column as a whole as total, that is divided into three: high, middle, and low level values (Figure 4) and their biases and RMSE with respect to ISCCP data (Rossow and Schiffer, 1999) for DJF, JJA and annual means (Table 3.1). We examined the simulated total cloud fraction that can be directly compared with satellite observations. The simulated total cloud fractions of MAC are larger than those of CTL but lesser than the observed. Its zonal distribution tracks the observed quite well. On this measure, MAC simulations produce lesser biases than the CTL. In comparison, column averaged cloud fraction biases in CTL are negative globally. Whereas MAC biases are also negative (except for polar regions), but they are half as much as CTL-biases except for the tropics. If the simulated cloud fraction is far off, the only way to get reasonable CRE is to tune cloud water or scaling the cloud fraction and/or their optical properties; while MAC uses cloud water path scaling, CTL performs convective cloud fraction scaling (see Table 1). Whereas CTL total clouds are consistently less than observed, MAC total clouds are similar to CTL in the tropics but larger than CTL in the higher latitudes (Figure 4a) and get even more than the observed in Polar Regions, a bias that has been highlighted before. Further details of high middle and low level clouds are as follows.

High clouds are equally robust and realistic in both CTL and MAC simulations except for the Polar Regions, where MAC high clouds show larger bias than the CTL (Figure 4b). On seasonal time-scales the biases do look quite different. Some biases of lesser than observed high cloud over north of India and western United States, and Argentina are common to both MAC and CTL simulations in DJF as well as JJA (not shown) leading to discernible signatures in the annual averages. Over the oceans, MAC does better than CTL, which overestimates high clouds. MAC mid-level clouds are much more realistic than those of CTL clouds at most places (Figure 4c). The mean RMSE errors of MAC (CTL) for DJF, JJA, ANN averages are smaller (larger) *vis-a-vis* ISSCP data as observations (see Table 3). Generally, CTL produces lesser than observed mid-level clouds. On low level clouds, MAC does a better job than CTL between 30S to 30N, but at higher latitudes MAC shows huge biases particularly in the Polar Regions where observations are not so reliable. Regardless, this makes low level cloud fractions of MAC somewhat inferior. Specifically, large biases in low-level cloud fractions at high latitudes are seen in all the seasons as well as in the annual means. CTL simulations produce lesser than observed low-level clouds, but they get better at higher latitudes (Figure 4d). In summary, clouds above 400hPa, called high clouds, are more than observed in both MAC and CTL simulations in both DJF and JJA seasons. In DJF, MAC (CTL) simulates about -0.3 % (0.7%) bias in the observed high clouds fraction of about 22%. In JJA too both MAC (CTL) simulate 0.5 % (1.3%) more high clouds and those biases are reasonable in GCM applications. Perhaps RAS, the basic convective scheme of both the CTL and McRAS-AC cloud scheme is responsible for such close similarity in cloud fractions in the tropics. A word of caution about ISSCP data is in order here. Its retrieval algorithm is unable to detect very thin cirrus; therefore its bias is towards lesser deep clouds and could explain high cloud biases as a spurious model deficiency.

The differences in the middle level, 700-400hPa, clouds are very much better in MAC *vis-à-vis* CTL. MAC biases are 2.2% for DJF and 1.5% in JJA versus -10.3% for DJF and -10.3% for JJA for CTL simulations. MAC scheme started producing more mid-level clouds after melting of snowfall at 0°C was introduced (Sud and Walker, 2003b). The snow melts around 500hPa in the tropics, produces an inversion that debars cumulus towers from penetrating through it. We also like to point out that mid-level cloud fraction in the ISSCP data may be too large (Chen and DelGenio, 2008) because the mid-level clouds percentages are almost same as high clouds percentages, but for now MAC simulates them and our radiation balances

suggest that cumulus congestus and mid level detrainment by high latitude cumulus clouds (Johnson et al., 1999) may be reasonable; however, the fall velocity of an embryonic hydrometeors is chosen for optimal estimates of cloud water (Sud and Lee, 2007). Even though both large-scale schemes use Slingo and Ritter (1987) type of critical relative humidity dependence for onset of stratiform clouds, the McRAS-AC determines only its tendency and not the amount (Sud and Walker, 1999a) as well as employs moist convection associated with stratiform clouds as an additional upgrade (Sud and Walker, 2003b). The latter would tend to increase the cloud fraction and its vertical correlation that shows up in the CRE analysis of Oreopoulos et al. (2012). MAC simulates almost 50% more low level clouds and those are all in high latitude regions. Similar high latitude biases in the CTL case are half as much. Overall, CTL simulated PBL clouds are about 4% less than the observed. However, in the tropics, MAC simulation is still as good. McRAS-AC module in all the past applications had a PBL cloud scheme that was based on dry convection and was linked to surface fluxes. In GEOS-5 GCM application used in MAC simulation, we rely on the PBL cloud scheme of the baseline GEOS-5 GCM. There seems to be need for reworking on the PBL clouds. In the regions with moist convection, moisture exits near the top of the PBL through dry convection but at high latitude with little or no convection, the moisture saturates the PBL and makes excessive PBL clouds. For example, in the Polar Regions, often precipitation emerges as tiny snow particles from the ice fog falling out of clear sky (diamond dust; Greenler, 1999). Our cloud model, McRAS-AC, may be identifying it as fully cloudy because local RH of the ambient atmosphere exceeds the saturation vapor pressure for ice, the criteria used to identify a large scale cloud in the model. Moreover PBL clouds develop over a long period of time and that gives them more time to entrain the aerosols into the turbulent plume. These are some of the ideas that can mitigate the high latitude cloud biases of McRAS that reflect in MAC simulations.

4.2.2 Total Cloud Water Path

The geographical distribution of total cloud water path (= sum of liquid plus ice water paths) simulated by MAC and CTL are shown in Figure 5. First, CTL biases are consistently negative in the high latitude regions and positive in the tropics. Most of the positive moisture biases are in the tropics, but still it is not able to counter the high latitude negative biases (see Table 3 for means and RMSEs). However, since the effective radii of cloud drops are

prescribed in CTL, it uncouples the cloud mass and number density from the cloud water budget and allows the modeller to optimize the results by tuning. Indeed the MAC simulation too has its biases. Its RMSEs are similar to those of CTL whereas its biases are better connected with the cloud water path. Too high total and liquid cloud water path is due to high water content in the storm tracks along the North Pacific Currents and the Gulf Stream over the Eastern boundaries of the Asian and North American continents. This bias is also reflected in the annual averages. The DJF biases are much smaller although the RMSE are not. This is mostly related to negative biases in Polar Regions, less than observed cloud water path in convective regions, lack of stratus clouds off the west coast of North and South America.

4.2.3 Liquid Cloud Water Path

The simulated liquid cloud water path is shown in Figure 6. Here OBS stands for SSM/I dataset from Greenwald et al.(1993) and Weng and Groudy,1996 which is good for oceans only. This has a distinctly different pattern than the total water path. Its mean statistics are better for MAC than CTL, while its RMSEs are not. Evidently, MAC produces less cloud water in the ITCZ, SPCZ in DJF, JJA and ANN averages; in other words, McRAS-AC generates more than observed precipitation in convective areas. Once that happens, both mass and number densities of cloud water reduce proportionally. Moreover, our analysis of fractional cloudiness shows that low level cloud fractions are more than the observed; therefore large water content in the stratiform regime and smaller particle sizes may also have contributed to this bias. However, adjusting the tuneable parameters of the scheme can potentially ameliorate this problem. On other specifics, in DJF there is too much liquid as well as total water in the 40-60S region of roaring winds. In fact, as the total cloud water bias reverses in JJA while the liquid cloud water still has a positive bias, we infer that the ice amount over the region in JJA is too small and that points to lack of IN and a delayed Bergeron process which waits to kick in until sufficient IN are available for water vapour to deposit on. This may well be related to lack of ice nucleating aerosols. Since ice is also an absorber of solar radiation, lack of ice in the clouds near the boundary layer may be one of the causes for the bias in solar absorption, which can only appear in DJF because the solar radiation at 40-60S latitudes is much smaller in JJA. Low cloud water path off the west coast of Americas in JJA is expected lacking the boundary layer stratus and that indeed happens in both MAC and CTL simulations. The liquid water content in the storm track regions from

1 Asia to west coast of North America (over the ocean) has a strong positive (negative) bias for
2 MAC (CTL). In fact if we examine the total water bias over the Gulf Stream and North
3 Pacific Current, the large positive bias in liquid and total cloud water in MAC simulation is
4 notable. This is related to large-scale clouds and presumably high aerosol content of the
5 ambient air mass that make precipitation rate too low.

7 **4.2.4 Sensitivity of Cloud Water to Aerosols**

8 A one year test simulation is made with interactive aerosols generate by the GOCART model
9 instead of the climatologically prescribed aerosols generated by the same model. The
10 interactive run reduces the aerosols within the storm in the storm track regions. Rain storms
11 not only remove the activated aerosols as CCN and/or IN through precipitation, but also
12 scavenge the inactivated ones through wash down, which is difficult to parameterize. In the
13 one year test, the high cloudiness and reflectivity bias of the clouds in the storm track regions
14 are greatly reduced giving us hope that the problem can be solved without a major research
15 effort (Figure 7).

17 **4.3 Cloud Particle Effective Radii**

18 The effective radii of ice and liquid cloud particles of MAC and CTL simulations are
19 compared against satellite data (Platnick et al., 2003). It must be pointed out that the
20 validation satellite data based on radiances is unable to see the entire vertical distribution of
21 cloud particles and their effective radii and therefore these radii are based on what the
22 instrument sees near the top. Figure 8 shows MAC and CTL effective radii for liquid and ice
23 cloud particles. The liquid effective radii of MAC simulation are in the range of 10-18 μm
24 with a global average of 14 to 14.4 μm in DJF and JJA seasons. It is too small by 1-1.5 μm ,
25 which is well within the spread of the observations; inferring the same from empirical
26 relations used in CTL, the values are in the 9-14 μm range with global average value of 10.1
27 to 10.5 μm for DJF and JJA respectively. Thus the CTL effective radii are about 30% smaller.
28 Indeed MAC is also biased somewhat on the smaller size, but the size depends upon the
29 aerosols activation and we believe, the input aerosols easily may have more than 5-10%
30 biases globally because their numbers are not well validated over the oceans. The fact that we
31 get liquid effective radius so close to observation shows that on this measure liquid aerosol

parameterization of MAC is as good as it can be expected of a realistic cloud model. Because of the assumptions about the sub-grid scales, and having seen the biases in clouds, the simulated zonal averages effective radii are as reasonable as one can hope to get in a GCM, whereas the prescribed effective radii in CTL runs are biased much more.

The simulated effective radii of cloud ice particles 24-42 μm with an average 28.3 to 29.9 μm for JJA and DJF respectively. Clearly MAC simulates larger effective radii but again it is about 10% or 3 μm too large and that too is well within the observational spread. In fact 3 μm in 30 μm can be easily explained by the range of variations between the effective and volume radius of ice particles. Again in CTL, the empirically estimated ice particle effective radius is $\sim 3 \mu\text{m}$ less than the observed, however, its zonal biases tell us that polar ice clouds have problem and that is consistent with their low number and large particle size. The RMSE errors of MAC are twice as large but that is to be expected because MAC numbers, being actual predictions, have a large spread whereas CTL values do not; (see Figure 8). Based on these results, MAC is simulating liquid and ice cloud effective radii reasonably well and is ready to perform as an aerosol-cloud-radiation interaction model with its current cloud physics. The grid average liquid and ice particle numbers are about 40 and 3.8 cm^{-3} with corresponding in-cloud values of (~ 90 and 10 cm^{-3}). There are no observed values for these but judging by the radiation imbalances at the top of the atmosphere, we assume that McRAS-AC simulated numbers have large zonal biases that may be aerosol related.

4.5.1 TOA radiation budget

In this subsection we assess briefly the verisimilitude of the radiation budget produced by the 10-yr simulations of GEOS-5 with the two cloud schemes. We compare model simulated TOA LW and SW zonal fluxes to their counterparts from CERES products (Loeb et al. 2009, CERES data set EBAF 2.6). Figure 9 shows for DJF, JJA, and ANN fields while global mean biases and RMS errors are displayed in Table 3. Assessments of deficiencies in the simulated cloud fields that lead to discrepancies between the simulated and the observed radiative fields are mostly left for the next subsection which frames the discussion in terms of cloud radiative effects (CRE).

The zonal-average radiation plots shown in Figure 9 indicate that for the most part, MAC matches OBS better than CTL. As will be discussed further later, while its tropical convective clouds have too little cloud water/ice and somewhat lower height, the resulting outgoing

longwave radiation (OLR) and absorbed shortwave radiation (ASW) are closer to observations than the CTL whose overactive convection yields too much reflected SW and too little OLR. MAC is less skillful in midlatitudes, however, with too much ASW in the SH summer (discussed extensively below) and too much OLR in the NH summer.

Overall, both schemes are in reasonable agreement with observations in terms of global mean OLR (Table 3), but MAC RMSE values are better by $\sim 2 \text{ Wm}^{-2}$ for both seasonal and annual averages, indicating larger spatial error cancellations for CTL. The annual averages of global ASW are about the same for both cloud schemes, and about $2.5 - 3.0 \text{ Wm}^{-2}$ larger than the observations. However, summer and winter global values differ substantially between the two schemes. MAC's ASW differs by $\sim 17 \text{ Wm}^{-2}$ between DJF and JJA while the corresponding differences in both observations and CTL are about half. Again, this is a result of deficient simulation of SH midlatitude marine clouds by MAC (the reasons for this bias and possible solutions are discussed later) making the RMSE slightly worse than CTL in DJF (Table 3). The same deficiency impacts also the global net TOA flux which is $\sim 9 \text{ Wm}^{-2}$ too high for MAC in DJF compared to the CERES. The global net TOA flux for JJA is within $\sim 1 \text{ Wm}^{-2}$ of observations for both MAC and CTL, but the DJF error of MAC is too large, yielding a substantial excess of 8.5 Wm^{-2} in annual global net TOA radiation. Our simulations are not much affected by this large energy imbalance because of externally prescribed SSTs. The RMSEs of net TOA radiation are worse for MAC than CTL for DJF, but are better for JJA, and about the same for ANN. Nevertheless, taking all radiation quantities into account, and focusing on their RMSEs (which are not affected by spatial cancellations), MAC generally produces radiation fields that are closer to observations than CTL. This is reaffirmed in the next subsection which examines cloud radiative effects.

4.5.2 TOA Cloud Radiative Effect

A well-established way for assessing the influence of clouds on the radiation budget is via the cloud radiative effect (CRE), a quantity also popularly known as cloud radiative forcing (Harrison et al. 1989). CRE for either solar/shortwave (SW) or thermal infrared/longwave (LW) radiation is defined as:

$$CRE_{LW,SW} = F_{LW,SW}^{cld} - F_{LW,SW}^{clr} \quad (1a)$$

which can also be recast as

$$CRE_{LW,SW} = C_{tot} (F_{LW,SW}^{ovc} - F_{LW,SW}^{clr}) \quad (1b)$$

under the assumption that the cloudy sky flux can be written as the linear combination of clear and overcast fluxes. In the above, F is the net downward (i.e., downward minus upward) flux (LW or SW), the superscripts *clr* designates clear (cloud-free) skies, *clt* designates all-sky conditions (containing a mixture of cloudy and clear skies), and *ovc* designates overcast skies (100% cloud fraction); C_{tot} is the total vertically projected cloud fraction which in the AGCM depends on individual layer cloud fractions and the cloud overlap assumptions. While both definitions can be used for analyzing observational data, the model CRE always comes from eq. (1a). Nevertheless, eq. (1b) is preferable for *interpreting* AGCM CRE. For two different cloud schemes producing the same C_{tot} , the CRE differences mainly arise from their water path/effective radius differences (their combined effect is captured by the cloud optical depth) in the SW, and cloud top height differences in the LW (although optical depth differences also play some role at low values of optical depth) through their effect on F^{ovc} .

The CRE as defined above can be calculated at either TOA or at the surface. Here we only show TOA results for which more reliable observed values are available. In the SW, the CRE TOA is usually negative because the net (absorbed) flux for cloudy skies is smaller than for clear skies. In the LW, the TOA CRE is usually positive because the upward TOA flux is greater under clear skies than cloudy skies (the downward flux is zero in both cases). The CRE of net radiation is, $CRE_{net} = CRE_{SW} + CRE_{LW}$, and can be positive or negative depending on cloud type. Measurements of TOA CRE are readily available from CERES, among other sources, and can be used for model evaluation. We use the EBAF v. 2.6 of the CERES data set (Loeb et al. 2009).

In an earlier paper, Oreopoulos et al. (2012) showed that for diagnostic radiation calculations with a different radiation scheme, the TOA CRE and its sensitivity to the vertical distribution of clouds was very different for the CTL and MAC clouds. Based on results of Oreopoulos et al. (2012) we naturally expected substantial CRE differences between MAC and CTL. The TOA CRE_{LW} differences between observations and the two model runs are shown in Figure 10. In this plot as well as similar ones that follow for CRE_{SW} and CRE_{net} , red and blue colors represent positive and negative biases with color intensity proportional to the magnitude of the bias. The lighter shade of colors for MAC minus OBS compared to CTL minus OBS is

indicative of smaller biases for MAC, and this is especially true over the Pacific. The CRE_{LW} biases in both simulations are consistent with those of cloud fraction bias discussed earlier in subsection 4.2.1. In the ITCZ region, MAC exhibits smaller CRE_{LW} than observations, probably because its convective clouds are too low or too thin, while CTL exhibits the opposite behavior, i.e., larger than observed CRE_{LW} , suggesting that convective clouds in CTL may be too high and/or too thick and too spatially extensive. In general, the MAC underestimates are lower than the CTL overestimates. Lower cloud tops in MAC may be due to the influence of quadratic entrainment in McRAS-AC (and neglect of convective height increase by freezing of cloud ice and precipitating hydrometeors) versus linear in the standard RAS of the GEOS-5 GCM (Sud and Walker, 2003a). Larger entrainment aloft will reduce the in-cloud moist static energy and will keep them shallow. In fact, when we examine all the places with abundance of convective clouds, the simulated CRE_{LW} in CTL is consistently too large suggesting that cloud tops are too high or the cloud free areas are too few or too small. Because lesser entrainment aloft will need lesser cloud mass to neutralize the cloud work function above the critical value, which would reduce the cloud fraction and mitigate the lesser CRE_{LW} biases as opposed to making them worse. Despite the previously mentioned weaknesses in the simulation of southern midlatitude ocean clouds by MAC, CRE_{LW} biases are not as high because most of the clouds at these latitudes reside in the lower troposphere and do not have much influence on the CRE_{LW} . On the other hand, biases in the snow and ice covered polar regions (where observed CREs may be less reliable), both the positive and negative biases are generally larger in MAC than in CTL for reasons that remain currently unidentified.

Overall, the CTL scheme underestimates global CRE_{LW} by $\sim 4 \text{ Wm}^{-2}$ (Table 3) mainly because of the systematic underestimates in convective areas. The MAC simulation approaches the global observed value within $\sim 1.0\text{-}1.5 \text{ Wm}^{-2}$ and achieves better RMSE scores than CTL in both the seasonal and annual means by $\sim 1.5\text{-}3 \text{ Wm}^{-2}$. Figure 11 shows TOA CRE_{SW} radiation difference maps. CRE_{SW} fields of CTL minus OBS have deeper colors with more structure compared to those of MAC minus OBS. Large differences in the biases are evident in MAC and CTL over northern midlatitudes in JJA. But the most prominent MAC biases (underestimates) appear in DJF within the 40S-60S latitude zone where MAC produces too few CPNC that have consequently too large sizes (see Section 4.3.). Since the region is dominated by sea salt aerosols, we hypothesize that either these aerosols are not activated adequately, or the inferred particle numbers from the GOCART mass concentrations are too

low. To examine the impact of the latter possibility, we conducted one year run where we reduced the sea-salt aerosol diameter by 50% across the board resulting in an 8-fold increase in aerosol particle number density (APND). This is a reasonable test because GOCART simulates mass balances employing only the mass tendency as sum of sources, sinks, aerosol chemistry and advection; APND for different bins is estimated from volume radius and density that match the aerosol optical thickness. The 8-fold increase in the sea salt APND resulted in a TOA CRE_{SW} field very similar to that of the CTL (Figure 12). While this experiment isolated the cause of the bias, it cannot be considered a solution. Greater ice particle numbers can also be created by a physically based ice-cloud particle splintering algorithms. The region is predominantly in the rising branch of the Ferrell cell where winds are strong and gusty, consequently CPNC increases due to cloud particle colliding and shattering, ignored in the current version of McRAS-AC, can be significant. Another mechanism that would increase IPNC is liquid cloud particles glaciating sooner as opposed to being depleted by Bergeron-Findeison mass exchange between water drops and ice particles through evaporation-desublimation process. Eliminating the biases with better algorithms, would not only mitigate the CPNC biases over 40S-60S, but would have the potential benefit of eliminating CRE_{SW} biases elsewhere as well. We are actively working on a physically-based solution to this problem.

The similarity of some biases appearing in both simulations suggest either the influence of their common RAS (Moorthi and Suarez, 1981) heritage or other shared model deficiencies such as absence of boundary-layer stratus clouds, and excessive orographic precipitation. Wherever the diagnostics show significantly similar biases in MAC minus OBS and CTL minus OBS, a common cause, not related to aerosol-cloud interaction, is assumed to be the culprit. Regarding the positive biases (underestimates of CRE_{SW}) over the PBL stratus regions off the west coast of California and Peru, an ad hoc tuning of the PBL moisture transport in the vertical ameliorated this problem in a test version of GEOS-5 GCM, but a more physically sound alternative is needed. Such is the scheme of Bretherton and Park (2008) which was successful in simulating realistic stratus clouds off west coast of north and south America as shown in Kay et al. (2012). The current baseline GEOS-5 GCM lacks PBL stratus, and in this exercise, both MAC and CTL simulations exhibit similar CRE_{SW} biases due to this inherent flaw(s) in the model's PBL convection.

1 The positive CRE_{SW} biases in southern midlatitude oceans beneath the Ferrell cell between
2 40S-60S are big enough to cause a global mean underestimate of 5 Wm^{-2} in DJF when the SH
3 insolation peaks. For the same reason, for SH summer, MAC's RMSE is slightly larger than
4 CTL even though for JJA and ANN the RMSE is notably smaller for MAC. The global ANN
5 CRE_{SW} of MAC is 1 Wm^{-2} too low since the SH summer underestimate is larger than the NH
6 summer overestimate. CTL simulates better the summer SH, but has in general more bias
7 compensations as evidenced by the larger RMSEs in JJA and ANN.

8
9 The bias fields of CRE_{net} (Figure 13) reflect previously discussed issues: In areas where
10 CRE_{LW} is small, the CRE_{SW} biases take over, see for example the SH midlatitude oceans
11 (MAC) and PBL stratus areas (both simulations). MAC fares better in the intensely
12 convective regions: apparently its CRE_{SW} and CRE_{LW} underestimates largely cancel out
13 because they have opposite signs. On the other hand for the CTL the tropical overestimates of
14 CRE_{SW} are significantly larger than the overestimates of CRE_{LW} resulting in too strong (too
15 negative) CRE_{net} , thus implying that the region loses radiative energy at a rate larger than that
16 of CERES observations. Based on the global values of CRE_{net} alone (Table 3), one would be
17 tempted to conclude that CTL simulates better cloud fields than MAC. But much of the
18 agreement with CERES is fortuitous and results from cancellations between the SW and LW
19 CREs as well as spatial cancellations. Indeed, the MAC RMSEs of CRE_{net} are lower on both
20 seasonal and annual basis.

22 **4.6 Comments on the Statistics of Circulation**

23 At the outset, one notes that the MAC and CTL simulations are closer to each other than the
24 Satellite data "so called observations" each of which provides useful guidance for model's
25 biases but each data has its own uncertainties. We first like to determine where McRAS-AC
26 really made a difference and whether it is statistically significant and/or beneficial for the
27 climate forecast. We found some differences in the precipitation and circulation, but most of
28 them were quite local and without much large scale structure. Other differences were in
29 regions where the input data to the 4DDA analysis system are sparse, the analysis largely
30 supported the background model simulations; clearly, there the biases were lesser for CTL as
31 opposed to MAC because analysis used the baseline GEOS-5 GCM. Its example is 100 to 200
32 hPa temperatures. We decided to postpone this analysis for Part 2 of this paper or until some

large biases of McRAS-AC are removed. This will figure in our future research. Significant changes in precipitation in convective regions are the only easily interpretable differences between MAC and CTL and those were discussed in Section 4.1.2

5 Summary and Conclusion

We examined 10 year long simulations with the GEOS-5 GCM with prescribed SSTs from SST analysis (reference). One used the baseline model and one used the McRAS-AC cloud physics, which includes McRAS cloud physics developed by Sud and Walker (1999a) with follow-on upgrades (Sud and Walker, 2003a,b) to include aerosol-cloud-radiation interactions (Sud and Lee, 2007). The New McRAS-AC has Barahona and Nenes (2009a,b) ice nucleation that is substituted for Liu and Penner (2005) ice nucleation scheme. Results show:

- a) McRAS-AC (MAC) simulation produced as good circulation and precipitation fields as the baseline GEOS-5 AGCM (CTL) simulation. There are patchy areas of significant differences in the circulation and precipitation, but most of the major circulation features are very similar. Accordingly, it is difficult to say categorically which one is better. In the mean and RMSE biases of precipitation, MAC simulation is a little better. Nevertheless, large 40S-60S biases in radiative CREs and cloud water path over the storm track regions and missing low level stratus does not justify declaring MAC to be better than CTL. However, for addressing these issues, we have identified good strategies that are supported by the subsequent sensitivity tests. Specifically insufficient cloud particle numbers over the 40S-60S regions are related to extremely deficient sea salt aerosols as well as lacking cloud particle enhancement by collision and splintering. While the high cloud water path in the storm track region is related to inefficient wash-down of aerosols by precipitation over the storm track regions of the North Pacific Currents and the Gulf Stream.
- b) MAC simulated better surface and TOA short and longwave radiative fields and their CREs but again its potential benefits were largely mitigated by large biases in the aforementioned regions. There are several plausible options for eliminating these biases, but we need to determine, which of them are most defensible physically. Elsewhere MAC produced better cloud fractions, cloud and ice water paths.
- c) The original McRAS-AC application produced shallow clouds based on dry convection, but in the GEOS-5 GCM application it was dropped in favour of the current GEOS-5

GCM PBL physics. This compromise may be responsible for McRAS-AC simulating so poor PBL clouds in high latitudes and keeping the low level clouds close to the surface.

- d) The cloud particle effective radii for water (ice) clouds is reasonable (somewhat larger) as compared to the observations, but it is definitely better than the empirical estimates of the baseline GEOS-5 GCM. Cloud ice particle splintering has the potential to ameliorate this bias.

Recognizing that aerosol cloud radiation interaction parameterization is in its infancy and most of the present day models still have discernible biases in aerosol cloud interactions (Kay et al., 2012), we submit that McRAS-AC cloud scheme is able to perform as well as the baseline cloud scheme of the GEOS-5 GCM despite a few large regional biases that are potentially correctable but reduces its RMSEs of the key fields. At this time, the performance of McRAS-AC in GEOS-5 GCM is as good as the baseline GEOS-5 GCM, if not unequivocally better yet, consequently one can start using McRAS-AC modified GEOS-5 GCM for climate research in which the focus is on studying the CRE of clouds as opposed to waiting for next upgraded that can make McRAS-AC more realistic.

Biased CREs are the primary source of biased background circulation in a climate simulation. Sometimes the climate change problem has smaller radiative forcing anomalies than the model's biases, e.g., doubled CO₂ effects produce a mere 3-4 Wm⁻² radiative forcing anomaly, while models simulating its influences may have biases as large as 30 Wm⁻² in many regions. Realizing that even the juxtapositions of model-biases vary among the models, consensus among their climate predictions is unlikely. Increasing the size of the domain would help because the CRE biases often reduce in averaging and when the region becomes sufficiently large, the climate change causing radiative forcing anomalies may exceed the model's biases and hence the possibility of consensus increases. Its prime example is better consensus among models in the global means. But if our goal is to capture climate prediction at the regional scales, we must reduce the CRE biases as much as possible.

1
2
3
4

5 **Acknowledgements**

6 The authors thank *David Considine* , Manager Modeling and Analysis Program of Earth
7 Science Division at *NASA Headquarters* for supporting this research. Computational
8 resources were provided by a separate proposal to the NASA Centre for Climate Simulation
9 (NCCS).

10

1 References

- 2 Adler, R.F., G.J. Huffman, A. Chang, R. Ferraro, P. Xie, J. Janowiak, B. Rudolf, U.
3 Schneider, S. Curtis, D. Bolvin, A. Gruber, J. Susskind, and P. Arkin, 2003: The Version 2
4 Global Precipitation Climatology Project (GPCP) Monthly Precipitation Analysis (1979-
5 Present). *J. Hydrometeor.*, 4,1147-1167, 2003.
- 6 Abdul-Razzak , H., and Ghan, S. J.: A Parameterization of Aerosol Activation. Part 2:
7 Multiple Aerosol Types." *Journal of Geophysical Research. D. (Atmospheres)* 105:6,837-
8 6,844, 2000.
- 9 Abdul-Razzak H., and Ghan, S. J. : A Parameterization of Aerosol Activation. Part 3:
10 Sectional Representation." *Journal of Geophysical Research. D. (Atmospheres)* 107(D3):AAC
11 1-1 - 1-6., 2002.
- 12 Andreae, M.O., Rosenfeld, D.: Aerosol–cloud–precipitation interactions. Part 1. The nature
13 and sources of cloud-active aerosols. *Earth-Science Reviews, Volume 89, Issues 1–2, Pages*
14 *13-41, July 2008.*
- 15 Albrecht, B. A.: Aerosols, Cloud Microphysics, and Fractional Cloudiness, *Science* 245,
16 1227-1230, 1989.
- 17 Bacmeister, J. T., Suarez, M. J. and Robertson, F.: Rain re-evaporation, Boundary layer
18 convection interaction and Pacific rainfall patterns in an AGCM., *J. Atmos. Sci.*, 63, 3383-
19 3403, 2006. doi: 10.1175/JAS3791.1.
- 20 Barahona, D., and Nenes, A.: Parameterizing the competition between homogeneous and
21 heterogeneous freezing in cirrus cloud formation: polydisperse ice nuclei, *Atmos. Chem.*
22 *Phys.*, 9, 5933–5948, 2009a.
- 23 Barahona, D., and Nenes, A.: Parameterizing the competition between homogeneous and
24 heterogeneous freezing in cirrus cloud formation: monodisperse ice nuclei, *Atmos. Chem.*
25 *Phys.*, 9, 1–13, 2009b.
- 26 Bergeron, T.: On the physics of cloud and precipitation. *Proc. 5th Assembly U.G.G.I. Lisbon*,
27 Vol. 2, p. 156, 1935.
- 28 Bougeault, P. and Geleyn, J. F.: Some problems of closure assumption and scale dependency
29 in the parameterization of moist deep convection for numerical weather

prediction. METEOROLOGY AND ATMOSPHERIC PHYSICS, 40, Numbers 1-3, 123-135, 1996. DOI: 10.1007/BF01027471

Bell T.L., J. -M. Yoo, and M. -I. Lee.: Note on the weekly cycle of storm heights over the southeast United States *J. Geophys. Res.*, 114(D15201), 2009. doi:10.1029/2009JD012041

Bell T.L., D. Rosenfeld, and K.-M. Kim.: The Weekly Cycle of Lightning: Evidence of Storm Invigoration by Pollution *Geophys. Res. Lett.*, 36(L23805), 2009. doi:10.1029/2009GL040915

Bellouin, N., Rae, J., Jones, A., Johnson, C. , Haywood, J. and Boucher, O.: Aerosol forcing in the Climate Model Intercomparison Project (CMIP5) simulations by HadGEM2-ES and the role of ammonium nitrate, *J. Geophys. Res.* (2011), 116, D20206, doi:10.1029/2011JD016074.

Bretherton, C. S., and Park, S.: A new moist turbulence parameterization in the Community Atmosphere Model. *J. Climate*, 22, 3422-3448, 2009.

Chao, W., 2012. Correction of Excessive Precipitation over Steep and High Mountains in a GCM. *J. Atmos. Sci.*. Document (3475 kb). Accepted Nov., 2011.

Charlson R.J., Schwartz, S. E., Hales, J. M., Cess, R. D., Coakley, J. A., Hansen, J. E. and Hofmann, D. J. : Climate Forcing by Anthropogenic Aerosols *Science* 24 January 1992: Vol. 255 no. 5043 423-430, 1992. DOI: 10.1126/science.255.5043.423.

Chen, Y, and Del Genio, A.D : Evaluation of tropical cloud regimes in observations and a general circulation model, 2008. *Climate Dynamics* doi:10.1007/s00382-008-0386-6.

Chin, M., Ginoux, P. , Kinne, S. , Holben, B. N. Duncan, B. N. , Martin, R. V. , Logan, J. A. Higurashi, A. and Nakajima, T.: Tropospheric aerosol optical thickness from the GOCART model and comparisons with satellite and sunphotometer measurements, *J. Atmos. Sci.* 59, 461-483, 2002.

Chou, M.-D., M. J. Suarez, X.-Z. Liang, and Michael M. H-Yan.: A Thermal Infrared Radiation Parameterization for Atmospheric Studies. *Technical Report Series on Global Modeling and Data Assimilation*, NASA/TM-2001-104606, Vol. 19, 65 pp, 2003.

Chou, M.-D., Suarez M. J.: A solar radiation parameterization for atmospheric studies, *Technical Report Series on Global Modelling and Data Assimilation*, NASA/TM-1999-10460, Vol. 15, 52 pp., 1999.

1 Chou, M.D., Suarez, M.J., Ho, C.H., Yan, M.M.H. and Lee, K.T.: Parameterizations for cloud
2 overlapping and shortwave single-scattering properties for use in general circulation and
3 cloud ensemble models, *J Climate* 11, pp. 202-214, 1998.

4 Colarco, P., A. daSilva, M. Chin, and T. Diehl.: Online simulations of global aerosol
5 distributions in the NASA GEOS-4 model and comparisons to satellite and ground-based
6 aerosol optical depth *J. Geophys. Res.*, 115(D14207), 2010. doi:10.1029/2009JD012820

7 Cotton, W.R., and Pielke, R.A.: Human impact on weather and Climate, Cambridge
8 University Press, pp. 288, 1995.

9 DelGenio, A.D., Yao, M.S., Kovari, W. K., and Lo, K.W.: A prognostic cloud water
10 parameterization for global climate models, *J Climate* 9, 270-304, 1996.

11 Findeisen, W.: Die kolloidmeteorologischen Vorgänge bei der Niederschlagsbildung
12 (Colloidal meteorological processes in the formation of precipitation). *Met. Z.*, 55, p.
13 121, 1993.

14 Fountoukis C., and Nenes, A.: Continued development of a cloud droplet formation
15 parameterization for global climate models, *J Geophys Res-Atmos* 110(2005), D11212,
16 doi:10.1029/2004JD005591

17 Gettelman, A., Liu, X., Ghan, S. J., Morrison, H., Park, S., Conley, A. J., Klein, S. A., Boyle,
18 J., Mitchell, D. L. and Li, J.-L. F.: Global simulations of ice nucleation and ice
19 supersaturation with an improved cloud scheme in the Community Atmosphere Model, *J.*
20 *Geophys. Res.*, 115, D18216, 2010, doi:10.1029/2009JD013797.

21 Ghan S J, Abdul-Razzak, H., Nenes, A., Ming, Y., Liu, X., Ovchinnikov, M, Shipway, B.,
22 Meskhidze, N., Xu, J., and Shi, X.: "Droplet Nucleation: Physically-Based Parameterization
23 and Comparative Evaluation." *Journal of Advances in Modeling Earth Systems* 3: Article No.
24 M10001, 2011. doi:10.1029/2011MS000074

25 Ghan S and coauthors.: A comparison of single column model simulations of summertime
26 midlatitude continental convection *J. Geophys. Res. - Atmos.*, (D2), 105, 2091-2124, 2000.

27 Gibbs, J. W.: "On the Equilibrium of Heterogeneous Substances, Part -1" Transactions of the
28 Connecticut Academy of Arts and Sciences III, 108-248, 1876.

29 Gibbs, J. W.: "On the Equilibrium of Heterogeneous Substances, Part -2" Transactions of the
30 Connecticut Academy of Arts and Sciences III, 343-524, 1878.

1 Greenler, R.: *Rainbows, Halos, and Glories*. Milwaukee: Peanut Butter Publishing. pp. 195,
2 1999, pp. [ISBN 0-89716-926-3](#).

3 Greenwald, T. J., Stephens, G. L., Haar, T. H. V., and Jackson, D. L.: A physical retrieval of
4 cloud liquid water over the global Oceans using Special Sensor Microwave/Imager (SSM/I)
5 observations, *J. Geophys. Res.*, 98, 18471–18488, 1993.

6 Gupta, S. K., Ritchey, N. A., Wilber, A. C., Whitlock, C. H., Gibson, G. G. and Stackhouse,
7 P. W.: A climatology of surface radiation budget derived from satellite data. *J. Climate*, 12,
8 2691–2710, 1999, doi:10.1029/2009JD013797

9 Gunturu, U. B.: *Aerosol-Cloud Interactions: A New Perspective in Precipitation Enhancement*
10 Ph.D. Thesis, Department of Earth, Atmospheric and Planetary Sciences, MIT, pp. 186, 2010.

11 Han, Q., Rossow, W. B., and Lacis, A. A.: Near-global survey of effective droplet radii in
12 liquid water clouds using ISCCP data. *J. Clim.*, 7, 465–497, 1994.

13 IPCC, *Climate Change: The Physical Science Basis*. Contribution of Working Group I to the
14 Fourth Assessment Report of the Intergovernmental Panel on Climate Change [Solomon, S.,
15 D. Qin, M. Manning, Z. Chen, M. Marquis, K.B. Averyt, M. Tignor and H.L. Miller (eds.)].
16 Cambridge University Press, Cambridge, United Kingdom and New York, NY, USA.

17 Karl, Thomas R. and Trenberth, K. E.: Modern Global Climate Change, *Science* : Vol.
18 302 no. 5651 pp. 1719-1723, 2007. DOI: 10.1126/science.1090228.

19 Johnson, R. H., Rickenbach, T. M., Rutledge, S. A., Ciesielski, P. E., and Schubert, W. H.:
20 Trimodal Characteristics of Tropical Convection. *J. Clim.*, 12, 2397–2418, 1999. doi:
21 10.1175/1520-0442(1999)012<2397:TCOTC>2.0.CO;2.

22 Khairoutdinov, M. F., and Y. L. Kogan.: A new cloud physics parameterization in a large-
23 eddy simulation model of marine stratocumulus. *Mon. Wea. Rev.*, 128, 229-243, 2000.

24 Kim M. -K., K. -M. Lau, M. Chin, K.-M. Kim, Y. C. Sud, and G.K. Walker.: Atmospheric
25 teleconnection over Eurasia induced by aerosol radiative forcing during boreal spring.: *J.*
26 *Climate* ., 19, 4700-4718, 2006.

27 Kim K.M., Lau, K. M., Sud, Y.C, and Walker, G. K.: Influence of aerosol radiative forcings
28 on the diurnal and seasonal cycles of rainfall over West Africa and Eastern Atlantic Ocean
29 using GCM simulations *Clim. Dynam*, 35, 115-126, 2010. doi:10.1007/s00382-010-0750-1

1 King, M. D. *et al.*, Cloud and aerosol properties, precipitable water, and profiles of
2 temperature and water vapor from MODIS, *Ieee T Geosc. Remote* 41, pp. 442-458, 2003.

3 Köhler, Hilding: The nucleus in and the growth of hygroscopic droplets. *Trans. Faraday Soc.*,
4 1936, 32, 1152-1161, 1936. DOI: 10.1039/TF936320115.

5 Koren, I., Altaratz, O., Remer, L., Feingold, G., and Heiblum, R.: Aerosol-induced
6 intensification of rain from the tropics to the mid-latitudes *Nature Geosciences*, *Online 15 Jan*
7 *2012*.doi:10.1038/ngeo1364

8 Krishnamurti T. N., Chakraborty, A., Martin, A., Lau, W.K., Kim, K.-M., Sud, Y. C., and
9 Walker, G. K.: Impact of Arabian Sea Pollution on the Bay of Bengal Winter Monsoon
10 Rains *J. Geophys. Res., Atmos.*, 114, 2009. D06213, doi:10.1029/2008JD010679.

11 Lau, W. K. M., and Kim, K.-M.: Fingerprinting the impacts of aerosols on long-term trends of
12 the Indian summer monsoon regional rainfall, *Geophys. Res. Lett.*, 37, L16705, 2010.
13 doi:10.1029/2010GL043255.

14 Lau, K. M., and Kim, K. M.: Does aerosol strengthen or weaken the Asian Monsoon? In
15 *Mountains: Witnesses of Global Change*, Ed. R. Baudo, G. Tartari, and E. Vuillermoz,
16 Elsevier, pp 340, 2007a.

17 Lau, K. M., Kim, K.M., Sud, Y.C., and Walker, G.K.: A GCM study of the response of the
18 atmospheric water cycle of West Africa and the Atlantic to Saharan dust radiative
19 forcing *Ann. Geophys.*, 27, 4023-4037, 2009.

20 Li, Z.-Q., Niu, F., Fan, J., Liu, Y. G., Rosenfeld, D., Ding, Y.: Long-term impacts of aerosols
21 on the vertical development of clouds and precipitation. *Nature Geoscience* 4, 888–894, 2011.
22 doi:10.1038/ngeo1313.

23 Lin, W. Y. and Zhang, M. H.: Evaluation of Clouds and Their Radiative Effects Simulated by
24 the NCAR Community Atmospheric Model Against Satellite Observations. *J. Clim.*, 17,
25 3302–3318, 2004.doi: 10.1175/1520-0442

26 Liu, X., and Penner, J.E.: Ice nucleation for global models, *Meteor.Zeitschrift*, 14, 499-514, 2005.

27 Liu X, Xie, S., Boyle, J., Klein, S.A., Shi, X., Wang, Z ., Lin, W., Ghan, S. J., Earle, M., Liu,
28 P., and Zelenyuk, A.: Testing Cloud Microphysics Parameterizations in NCAR CAM5 with
29 ISDAC and M-PACE Observations. *Journal of Geophysical Research. D. (Atmospheres)*
30 116:Article No: D00T11, 2011. doi:10.1029/2011JD015889.

1 Lock, A. P., Brown, A. R., Bush, M. R., Martin, G. M., and Smith, R. N. B.: A new boundary
2 layer mixing scheme. Part I: Scheme description and single-column model tests. *Mon. Wea.*
3 *Rev.*, 128, 3187–3199, 2000..

4 Loeb, N.G., Wielicki, B. A., Doelling, D. R., Smith, G. L., Keyes, D. F., Kato, S., Manalo-
5 Smith, N. and Wong, T.: Toward Optimal Closure of the Earth's Top-of-Atmosphere
6 Radiation Budget. *J. Clim.*, 22, 748–766, 2009. doi: 10.1175/2008JCLI2637.1.

7 Lohmann, U. : "Aerosol Effects on Clouds and Climate". *Space Sci Rev* 125 (1-4): 129–
8 137. Bibcode, SSRv..125..129L, 2006. doi:10.1007/s11214-006-9051-8.

9 Maloney, E. D., Hartmann, D. L.: The Sensitivity of Intraseasonal Variability in the NCAR
10 CCM3 to Changes in Convective Parameterization. *J. Climate*, 14, 2015–2034,
11 2000. doi.org/10.1175/1520-0442, 2001.

12 Molod, A. And Coauthors: GEOS-5 Atmospheric General Circulation Model: mean climate
13 development from MERRA to Fortuna, Tech. Memo., NASA Goddard Space Flight Center,
14 MD, pp 115, 2012.

15 Moorthi, S and Suarez, M.J.: Relaxed Arakawa-Schubert - a Parameterization of Moist
16 Convection for General-Circulation Models, *Mon Weather Rev* 120(1992), pp. 978-1002.

17 Morrison, H., and Gettelman, A.: A new two-moment bulk stratiform cloud microphysics
18 scheme in the NCAR Community Atmosphere Model (CAM3), Part I: Description and
19 numerical tests, *J. Clim.*, 21 (15), 3642–3659, 2008.

20 Nenes A, Ghan, S.J., Abdul-Razzak, H., Chuang, P., and Seinfeld, J. : Kinetic Limitations on
21 Droplet Formation. *Tellus Series B, Chemical and Physical Meteorology* 53:133-149, 2001.

22 Nenes, A. and Seinfeld, J. H.: Parameterization of cloud droplet formation in global climate
23 models, *J Geophys Res-Atmos* 108D7, 4415, 2003. doi: 10.1029/2002JD002911

24 Platnick, S. and Coauthors.: The MODIS cloud products: algorithms and examples from
25 Terra. *IEEE Trans. Geo. Rem. Sens.*, 41 (2), 459-47, 2003.

26 Pruppacher, H. R., and J. D. Klett.: *Microphysics of Clouds and Precipitation*, Second
27 Revised and Enlarged Edition with an Introduction to Cloud Chemistry and Cloud Electricity,
28 Kluwar Academic Publishers, pp. 954, 1997.

29 Quaas, J., Boucher, O., and Breon, F.-M.: Aerosol-cloud interactions in the LMDZ GCM and
30 in POLDER satellite data. *Geophy. Res. Abs.*, 5(2003), 30-1-2003.

1 Randall, D. A.: The Evolution of Complexity in General Circulation Models. In The
2 Development of Atmospheric General Circulation Models: Complexity, Synthesis, and
3 Computation, L. Donner, W. Schubert, and R. C. J. Somerville, Eds., Cambridge University
4 Press, 272 pp., 2010.

5 Rienecker M. M, Suarez, M. J., Todling R., Bacmeister J., Takacs L., Liu H.-C., Gu W.,
6 Sienkiewicz M., Koster, R. D., Gelaro, R., Stajner, I., and Nielsen, J. E.: The GEOS-5 Data
7 Assimilation System Documentation of Versions 1 5.0.1, 5.1.0, and 5.2.0. NASA/TM–2008–
8 2 104606, Vol. 27, 118 pp., 2008.

9 Roelofs, G.J., Stier, P., Feichter, J., Vignati, E., and Wilson, J.: Aerosol activation and cloud
10 processing in the global aerosol-climate model ECHAM5-HAM, *Atmos Chem Phys* 6, pp.
11 2389-2399, 2006.

12 Rosenfeld, D.: Suppression of rain and snow by urban and industrial air pollution, *Science*
13 287, pp. 1793-1796, 2000.

14 Rosenfeld, D. : "Aerosol-Cloud Interactions Control of Earth Radiation and Latent Heat
15 Release Budgets". *Space Sci Rev* 125 (1-4): 149–157,
16 2006. Bibcode 2006SSRv..125..149R. doi:10.1007/s11214-006-9053-6.

17 Rosenfeld, D., and T. Bell .: Why do tornados and hail storms rest on weekends? *J. Geophys.*
18 *Res. Atmos*, 116, D20211, 2011. doi:10.1029/2011JD016214

19 Rossow, W. B. and Schiffer, R. A.: Advances in understanding clouds from ISCCP. *Bull.*
20 *Amer. Meteor. Soc.*, 80, 2261-2288, 1999. doi: 10.1175/1520-0477.

21 Rotstayn, L. D, Ryan, B., and Katzfey, J.: A scheme for calculation of the liquid fraction in
22 mixed-phase stratiform clouds in large-scale models, *Monthly Weather Rev.*, 128, 1070–1088,
23 2000.

24 Seifert, A., and Beheng, K.D.: A double-moment parameterization for simulating
25 autoconversion, accretion and self collection, *Atmos Res* 59, pp. 265-281, 2001.

26 Seinfeld, J. H., Pandis, S. N.: Atmospheric Chemistry and Physics - From Air Pollution to
27 Climate Change (2nd Edition).. John Wiley & Sons. Pp 987, 2006.

28 Slingo, J.M.: The Development and Verification of a Cloud Prediction Scheme for the Ecmwf
29 Model, *Q J Roy Meteor Soc* 113, pp. 899-927, 1987.

1 Smith, R.N.B.: A scheme for predicting layer-clouds and their water content in a General
2 circulation model. Q.J.Roy.Meterol. Soc., Part B, 116: 435-460, 1990.

3 Sud Y.C., and Walker, G. K.: Microphysics of clouds with the relaxed Arakawa-Schubert
4 Cumulus Scheme (McRAS). Part I: Design and evaluation with GATE Phase III data J.
5 Atmos. Sci., (18), 56, 3196-3220, 1999a.

6 Sud Y.C., and Walker, G. K.: Microphysics of clouds with the relaxed Arakawa-Schubert
7 Cumulus Scheme (McRAS). Part II: Implementation and performance in GEOS II GCM, J.
8 Atmos. Sci., (18), 56, 3221-3240, 1999b.

9 Sud Y.C., and G.K. Walker, G. K.: New upgrades to the microphysics and thermodynamics of
10 clouds in McRAS: SCM and GCM evaluation of simulation biases in GEOS
11 GCM Proceedings of the Indian National Science Academy, Part-A, Physical Sciences(5) 69,
12 543-565, 2003a.

13 Sud, Y.C. and Walker, G. K.: Influence of ice-phase physics of hydrometeors on moist-
14 convection. Geophysical Research Letters 30(14), 2003b. doi: 10.1029/2003GL017587.
15 ISSN: 0094-8276.

16 Sud, Y.C., Mocko, D.M., and Lin, S. -J.: Performance of two cloud-radiation
17 parameterization schemes in the fvGCM for anomalously wet May and June 2003 over the
18 continental United States and Amazonia J. Geophys. Res. Atmos.(D6), 6201, 111, 2006.
19 doi:10.1029/2005JD006246

20 Sud Y.C., E.M. Wilcox, K. -M. Lau, G.K. Walker, X. -H. Liu, A. Nenes, D. Lee, K.-M. Kim,
21 Y. Zhou, and P.S. Bhattacharjee.: Sensitivity of Boreal-Summer Circulation and Precipitation
22 to Atmospheric Aerosols in Selected Regions, Part I: Africa and India *Annales Geophysicae*,
23 27, 3989-4007, 2009.

24 Sud Y.C., and Lee, D.: Parameterization of aerosol indirect effect to complement McRAS
25 cloud scheme and its evaluation with the 3-year ARM-SGP analyzed data for single column
26 models *Atmos. Res.*, , Issue 2, , 86, 105-125 10.1016/j.atmosres.2007.03.007, 2007.

27 Sundqvist, H.: Parameterization of condensation and associated clouds in models for weather
28 prediction and general circulation simulation. Physically-Based Modelling and Simulation of
29 Climate and Climatic Change, ed. M. E. Schlesinger, Kluwer Academic Publishers,
30 Dordrecht, the Netherlands, pp. 433-461, 1988.

- 1 Suzuki, K. *et al.*, A study of the aerosol effect on a cloud field with simultaneous use of GCM
2 modeling and satellite observation, *J Atmos Sci* , 61, pp. 179-194, 2004.
- 3 Tiedtke, M.: Representation of Clouds in Large-Scale Models, *Mon Weather Rev* 121, pp.
4 3040-3061, 1993.
- 5 Twomey, S.: The nuclei of natural cloud formation, II, The supersaturation in natural clouds
6 and the variation of cloud droplet concentration, *Geofis. Pura Appl.*, 43, 243249, 1959.
- 7 Twomey, S. : "Pollution and the planetary albedo". *Atmos. Environ.* 8 (12): 1251–6,
8 1974. doi:10.1016/0004-6981(74)90004-3.
- 9 Twomey, S. : "The Influence of Pollution on the Shortwave Albedo of Clouds" (PDF). *J.*
10 *Atmos. Sci.* 34 (7): 1149–52, 1977. Bibcode 1977JAAtS...34.1149T. doi:10.1175/1520-
11 0469(1977)034<1149:TIOPOT>2.0.CO;2.
- 12 Weng, F. Z. and Grody, N. C.: Retrieval of cloud liquid water using the Special Sensor
13 Microwave Imager (SSM/I), *J. Geophys. Res.*, 99, 25535–25551, 1994.
- 14 Wilber, A. C., Smith, G. L., Gupta, S. K., and Stackhouse, P. W.: Annual cycles of surface
15 shortwave radiative fluxes. *J. Climate*, 19, 535–547, 2006.
- 16 Wilcox E.M., Sud, Y.C. and Walker, G.K.: Sensitivity of Boreal-Summer Circulation and
17 Precipitation to Atmospheric Aerosols in Selected Regions, Part II: The Americas *Annales*
18 *Geophysicae*, 27, 4009-4021, 2009.
- 19 Wood, R., and C. S. Bretherton, 2004: Boundary layer depth, entrainment, and decoupling in
20 the cloud-capped subtropical and tropical marine boundary layer. *J. Climate*, 17, 3575–3587.
- 21 Xie, S. C., Cederwall, R.T., and Zhang, M.H.: Developing long-term single-column
22 model/cloud system-resolving model forcing data using numerical weather prediction
23 products constrained by surface and top of the atmosphere observations, *J Geophys Res-*
24 *Atmos* 109, D01104, 2004. doi:10.1029/2003JD004045.
- 25 Xie S. and coauthors.: Intercomparison and evaluation of cumulus parameterizations under
26 summertime midlatitude continental conditions *Quart. J. Roy. Meteor. Soc.*, (582), 128, 1095-
27 1136, 2002.

1 **Table 1. Parameterizations in GEOS-5 GCM and McRAS-AC Cloud Scheme (s)**

Model Specifications	Baseline GEOS-5 GCM	McRAS-AC in GEOS-5 GCM
Deep Convection	RAS (Moorthi and Suarez (1992)	McRAS (Sud and Walker,1999a)
Stratiform cloud	Smith (1990), Molod (2012)	Sud and Walker (1999a)
Precipitation liquid	Rienecker et al. (2008)	Sud and Lee (2007)
Precipitation snow	Rienecker et al. (2008)	Sundqvist (1988)
Rain evaporation	Bacmeister et al. (2006)	Sud and Molod (1988)
Cloud microphysics	Single moment microphysics	Double moment microphysics
Cloud Scaling	Convective cloud fraction scaled (Rinecker et al. 2008).	Cloud water Path scaled (Sud and Walker, 1999a)
Aerosol Effects	Direct effects only	Both direct and indirect effects.
CCN Activation	Not included	Fountoukis and Nenes (2005)
IN Nucleation	Not included	Barahona and Nenes (2009a)
Liquid Particle Number Concentration (LPNC)	CP Effectiv radius determined as a function of T and P	LPNC tendency budget of sources and Sinks.
Ice Particle Number Concentration (IPNC)	Not included; Effectiv radius determined as a function of T and P	IPNC tendency budget of sources and Sinks.
Cloud liquid mass	Emperical equation for cloud water nass fraction as a function of T	Solution of cloud liquid mass Tendency Eq. minus BF loss.
Cloud Ice mass	Total cloud mass minus liquid mass	Solution of cloud liquid mass Tendency Eq. minus BF loss.

2

3

4

5

6

1 Table 2. Descriptions of Simulation Experiments

Simulation Experiments	Descriptions	Years
Control Run (CTL)	GEOS-5 GCM standard moist physics	10
McRAS-AC Run (MAC)	GEOS-5 GCM with McRAS-AC	10
MAC run with half the sea salt particle size	McRAS-AC with half size sea salt (eight times number density or 8xSS)	1 year Test
Interactive GOCART with MAC	GOCART interactive with GEOS-5 McRAS-AC	1year Test

2

3

4 Table 3. Global mean MAC and CTL Simulation Fields versus Observations

Periods (left to right) Fields (top to bottom)	*OBS:Observed Mean			MAC: Mean/(RMSE)			CTL: Mean/(RMSE)		
	DJF	JJA	ANN	DJF	JJA	ANN	DJF	JJA	ANN
Precipitation (mm day ⁻¹)	2.68	2.71	2.68	2.89 (1.54)	3.01 (1.87)	2.92 (1.32)	2.84 (1.58)	3.05 (1.92)	2.89 (1.29)
Total Cloud Fraction	67.0	65.5	66.4	56.7 (17.1)	55.0 (16.6)	55.6 (15.8)	44.3 (25.6)	44.8 (24.8)	44.5 (24.3)
High Cloud Fraction	21.9	21.9	21.7	21.6 (8.9)	22.4 (9.3)	22.3 (6.6)	22.6 (8.9)	23.2 (9.8)	23.1 (7.6)
Middle Cloud Fraction	19.6	17.7	19.2	21.9 (9.3)	19.2 (7.4)	20.5 (6.7)	9.9 (13.3)	9.9 (10.8)	9.8 (11.5)
Low Cloud Fraction	24.9	26.6	25.6	37.0 (21.2)	35.4 (18.5)	35.9 (19.8)	22.0 (13.7)	22.8 (17.4)	22.2 (13.1)
Cloud Liquid Water Path (g m ⁻²)	84.3	85.8	84.3	76.6 (40.1)	84.2 (44.9)	79.4 (34.1)	72.9 (26.4)	74.5 (33.2)	72.4 (24.2)
Cloud Total Water Path (g m ⁻²)	89.9	90.5	88.2	92.1 (51.4)	107.0 (65.1)	98.3 (41.1)	77.2 (59/8)	82.4 (57.9)	77.8 (48.7)

Cloud-ice effective Radius (μm)	24.8	25.6	25.2	29.9 (8.8)	28.3 (9.3)	28.6 (7.1)	21.5 (4.5)	21.9 (6.8)	21.6 (4.4)
Cloud-drop effective Radius (μm)	15.2	16.3	15.6	14.3 (4.2)	14.4 (4.4)	14.0 (3.3)	10.1 (6.1)	10.5 (7.1)	10.3 (6.1)
Grid Average/In-cloud IPNC ($\# \text{ cm}^{-3}$)				4.1/ 10.6	3.5/ 9.4	4.1/ 10.7			
Grid Average/In-cloud LPNC ($\# \text{ cm}^{-3}$)				35.0/ 68.9	44.5/ 93.1	44.3/ 90.3			
OLR (W m^{-2})	236.9	243.3	239.7	236.0 (8.7)	242.0 (9.8)	238.6 (7.0)	237.4 (10.3)	245.8 (12.1)	241.1 (9.0)
ASW (W m^{-2})	244.5	235.7	240.5	252.2 (18.9)	235.3 (15.5)	243.3 (12.1)	246.7 (17.2)	239.0 (21.7)	243.0 (15.6)
Total TOA Rad. (W m^{-2})	7.6	-7.6	0.83	16.2 (17.5)	-6.6 (12.4)	4.7 (11.1)	9.3 (13.4)	-6.8 (16.3)	2.0 (11.2)
LW TOA CRE (W m^{-2})	25.9	26.3	26.2	24.5 (7.7)	25.4 (7.4)	25.3 (6.0)	21.6 (9.3)	22.2 (10.2)	22.2 (8.3)
SW TOA CRE (W m^{-2})	-51.6	-44.8	-47.3	-45.6 (17.9)	-46.7 (16.2)	-46.3 (12.2)	-50.8 (17.3)	-43.2 (20.9)	-46.4 (15.3)
Total CRE TOA (W m^{-2})	-25.6	-18.4	-21.1	-21.1 (16.9)	-21.3 (14.2)	-21.1 (11.3)	-27.8 (18.4)	-17.2 (21.0)	-21.7 (15.2)

1 * Datasets deployed

- 2 a) GPCP for Precipitation (Adler et al., 2003)
- 3 b) ISCCP for Clouds (Rossow, and Schiffer, 1999)
- 4 c) SSM/I for liquid water path (Greenwald et al., 1993)
- 5 | d) MODIS for effective radii and total water path (Platnick et al., 2003)
- 6 e) CERES for TOA Radiation (Loeb et al., 2009)
- 7 f) SRB for Surface Radiation (Wilber et al., 2006)

8

Figure Captions

Figure 1.: Cloud Physics and Microphysics of baseline GEOS-5 GCM and its modification to allow McRAS-AC to replace the relevant moist physics module of the GCM

Figure 2.: Simulated ten year mean precipitation (mm day^{-1}) for DJF(top) , JJA (middle), and Annual mean (bottom) in MAC and CTL runs (left 2 panels) and MAC minus OBS and CTL minus OBS (right two panels) ; GPCP data represents OBS.

Figure 3.: Statistically significant precipitation differences (mm day^{-1}) are color coded: MAC minus CTL for DJF (top) , JJA (middle), and Annual mean (bottom) using a 2-tailed student t-test.

Figure 4.: Ten year mean zonal average cloud Fractions for a) entire column atmosphere, b) 400hPa to top, c) 400-700 hPa, d) and 700hPa to surface in MAC and CTL simulations versus ISSCP and MODIS Climatology.

Figure 5.: Total Cloud Water Path for the full depth of the atmosphere in g m^{-2} for DJF(top) , JJA (middle), and Annual mean (bottom) in MAC and CTL runs and MAC minus OBS (left two panels) and CTL minus OBS (right two panels); MODIS data represents OBS.

Figure 6.: Same as Figure 5 except for Cloud Liquid Water Path; SSMI data represents OBS

Figure 7.: Total Water Path for JJA in g m^{-2} ; interactive aerosol chemistry minus GOCART.

Figure 8.: Zonal Average plots of a) ice and b) liquid cloud particle effective radius (μm). Different colors are used for Land, Ocean, and Total (colors legends are displayed in the Plots) for MODIS data (dotted), MAC simulations data (solid), and CTL simulations (gray) (note only one line for the prescribed value for CTL).

Figure 9.: Zonal average TOA OLR and TOA ASW in Wm^{-2} for DJF (top), JJA (middle), and ANN (bottom). The line colors used for MAC, CTL, OBS are shown in the middle panel.

Figure 10.: Distribution of simulated OLR minus OBS CRE TOA in Wm^{-2} . The rows have DJF (top), JJA(middle) and ANN (bottom). Right (left) columns are for CTL (MAC) data.

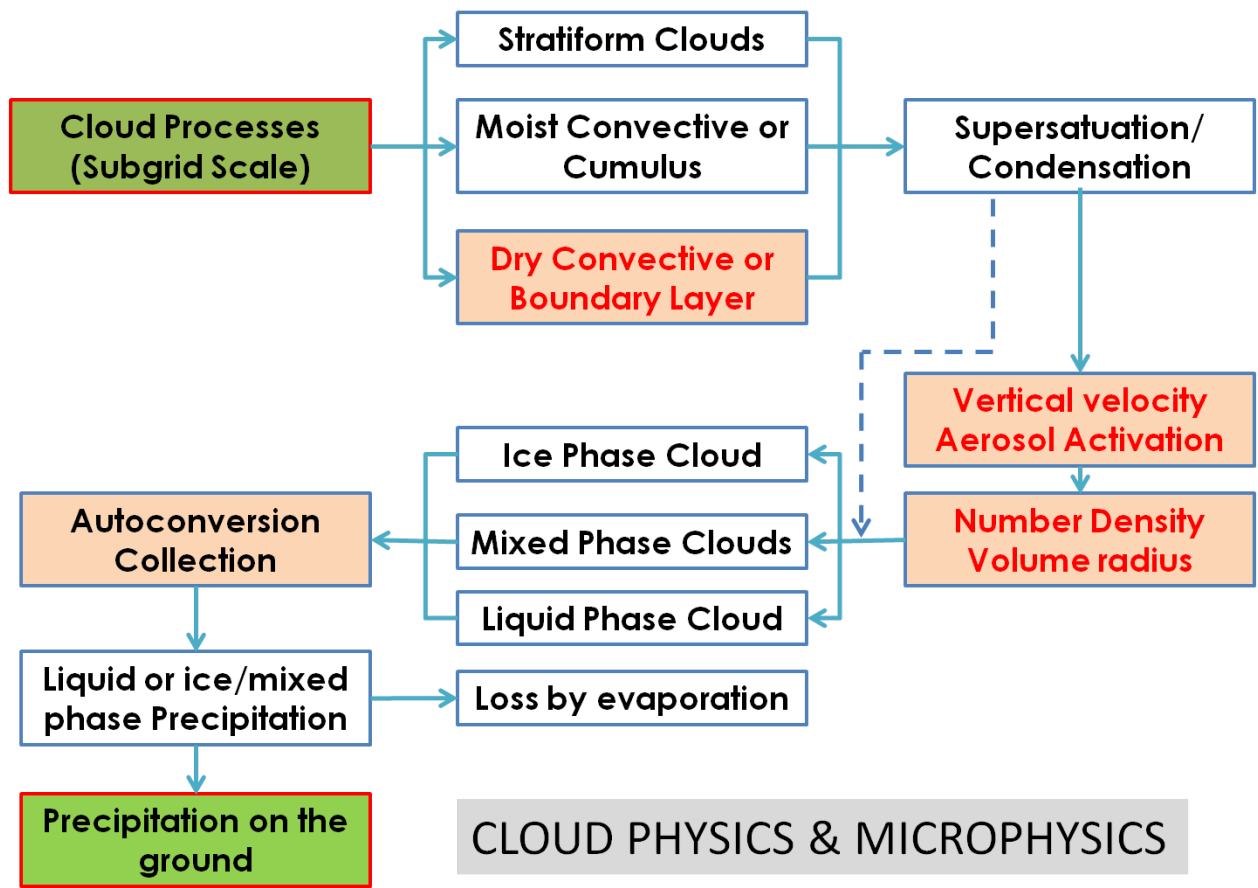
Figure 11.: Same as Figure 10, but for SWA CRE TOA in Wm^{-2} .

Figure 12.: DJF simulation for a year with MAC GCM using 8x the sea salt particles. Biases between the simulated minus observed SW CRE TOA are virtually gone.

1 Figure 13.: Simulated ten year mean TOA net radiation (Wm^{-2}) for DJF(top) , JJA (middle),
2 and Annual mean (bottom) by MAC and CTL runs (left 2 panels) and MAC minus OBS and
3 CTL minus OBS (right two panels) ; CERES data represents OBS.

4

1



2

3 Figure 1

4 Figure 1.: Cloud Physics and Microphysics of baseline GEOS-5 GCM and its modification to
5 allow McRAS-AC to replace the relevant moist physics module of the GCM

6

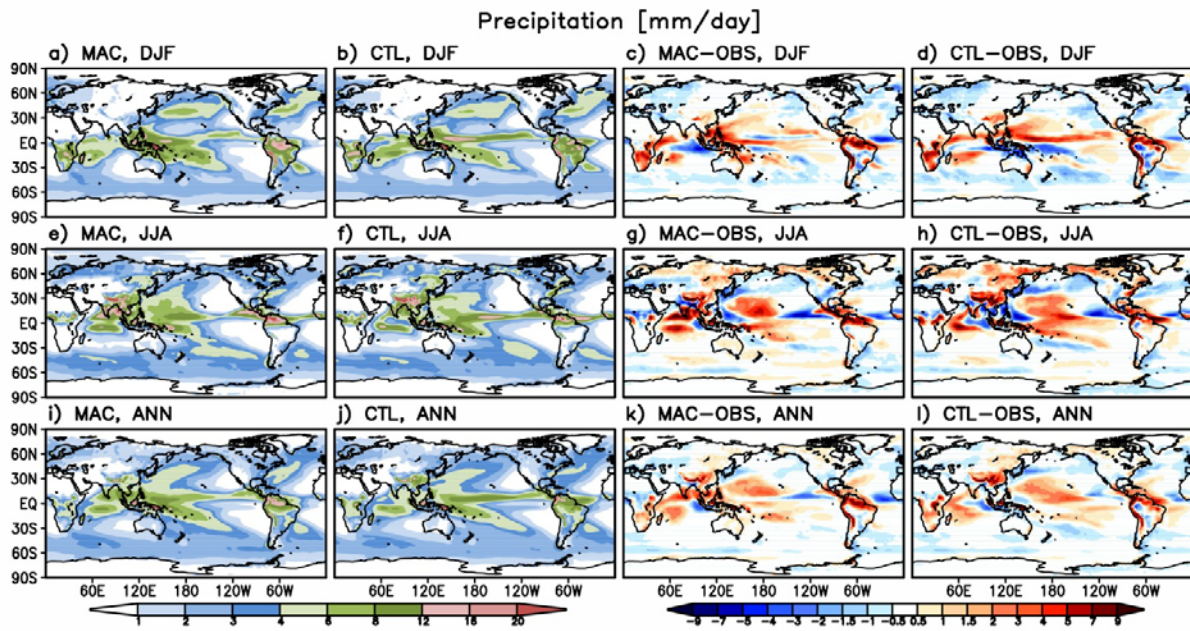
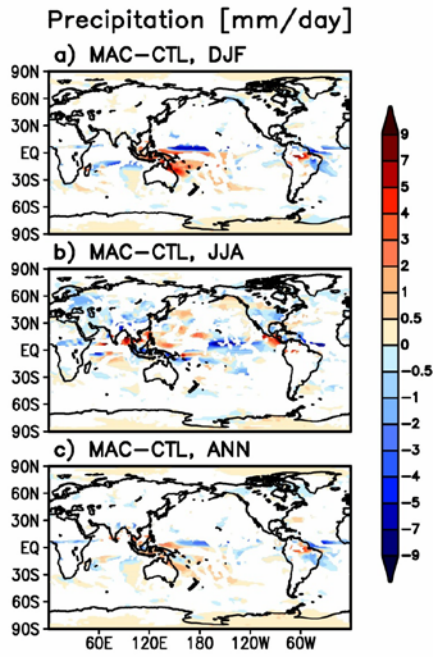


Figure 2

Figure 2.: Simulated ten year mean precipitation (mm day^{-1}) for DJF(top) , JJA (middle), and Annual mean (bottom) in MAC and CTL runs (left 2 panels) and MAC minus OBS and CTL minus OBS (right two panels) ; GPCP data represents OBS.

1



2

3 Figure 3

4 Figure 3.: Statistically significant precipitation differences (mm day⁻¹) are color coded: MAC
5 minus CTL for DJF (top) , JJA (middle), and Annual mean (bottom) using a 2-tailed student t-
6 test.

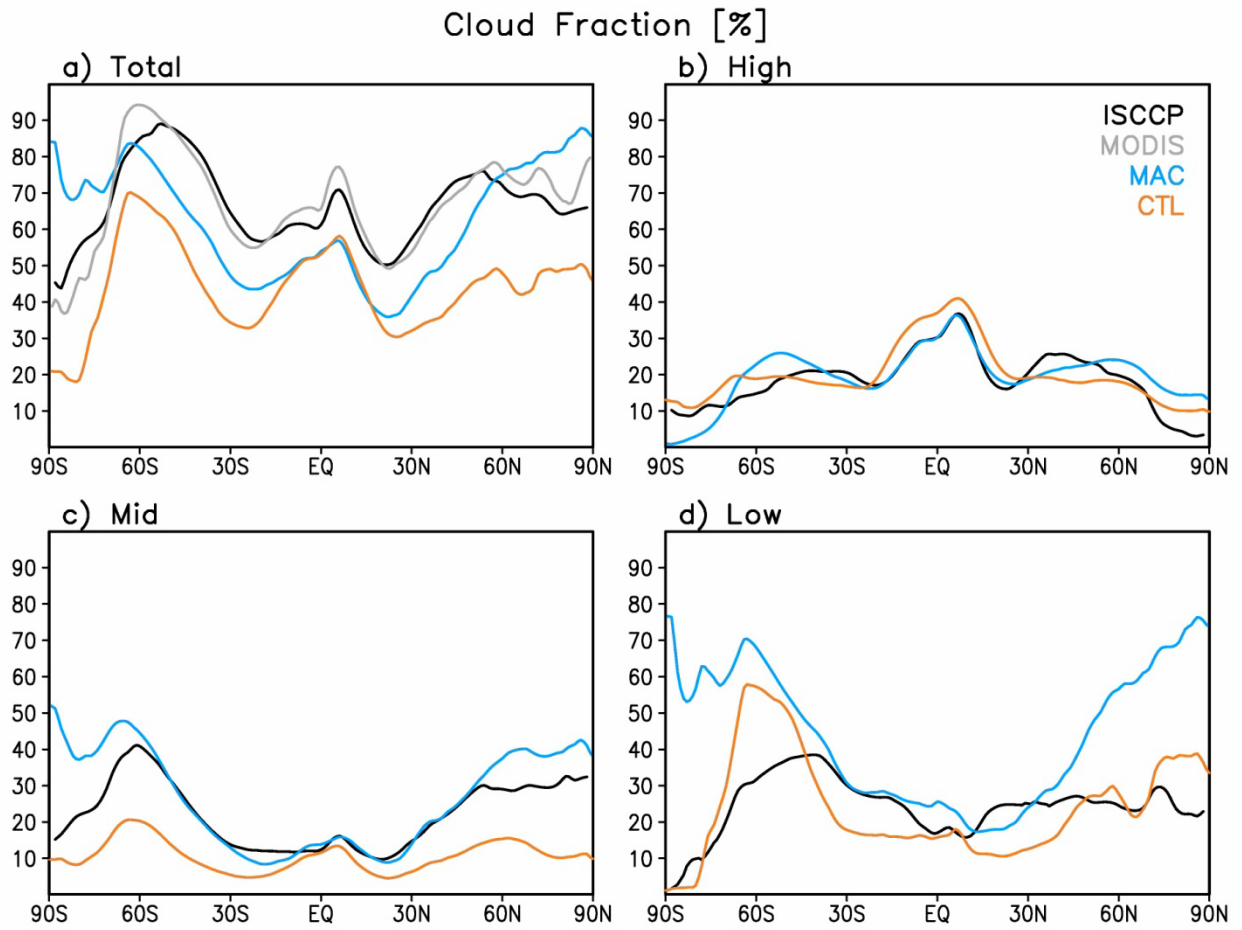


Figure 4

Figure 4.: Ten year mean zonal average cloud Fractions for a) entire column atmosphere, b) 400hPa to top, c) 400-700 hPa, d) and 700hPa to surface in MAC and CTL simulations versus ISSCP and MODIS Climatology.

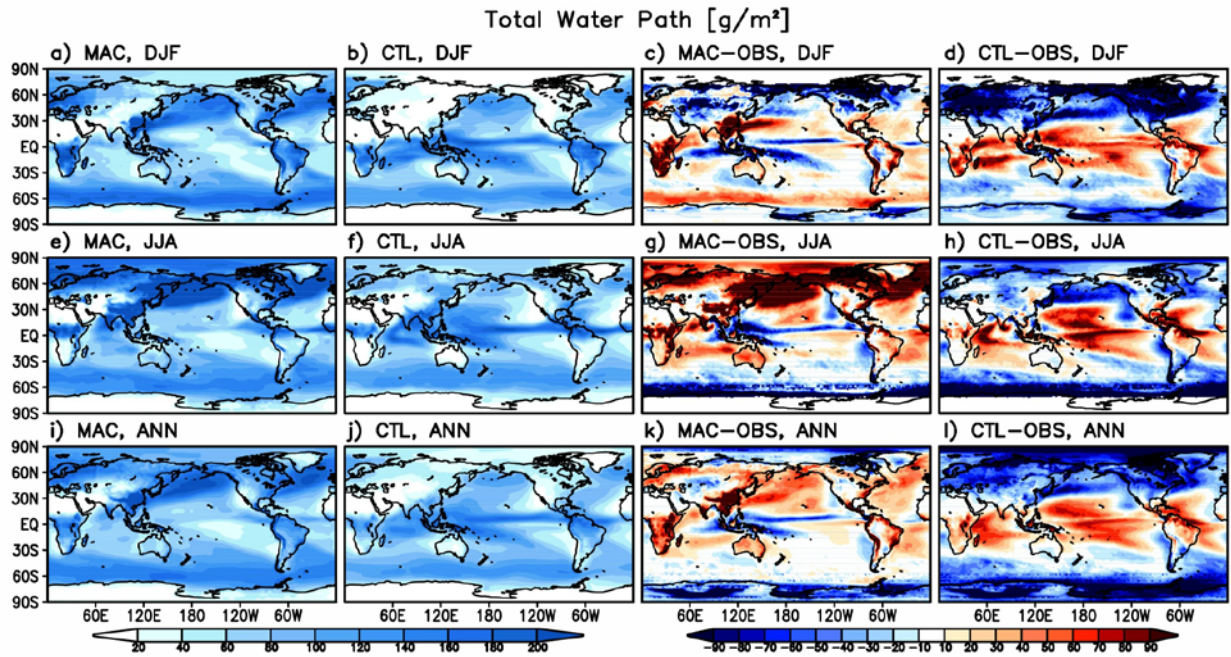


Figure 5

Figure 5.: Total Cloud Water Path for the full depth of the atmosphere in gm^{-2} for DJF(top) , JJA (middle), and Annual mean (bottom) in MAC and CTL runs and MAC minus OBS (left two panels) and CTL minus OBS (right two panels); MODIS data implies OBS.

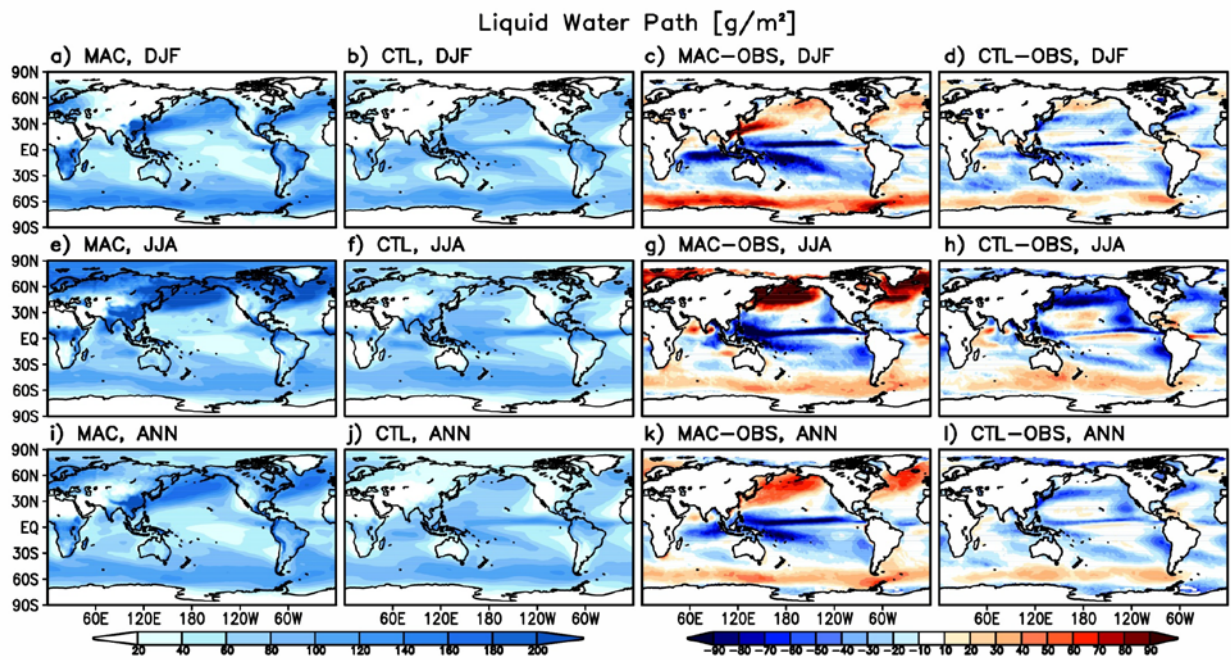


Figure 6

Figure 6.: Same as 3 except for Cloud Liquid Water Path; SSMI data represents OBS

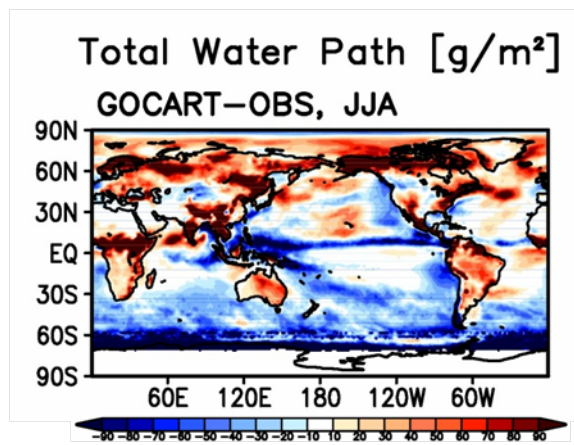


Figure 7

Figure 7.: Total Water Path for JJA in g m^{-2} ; interactive aerosol chemistry minus GOCART.

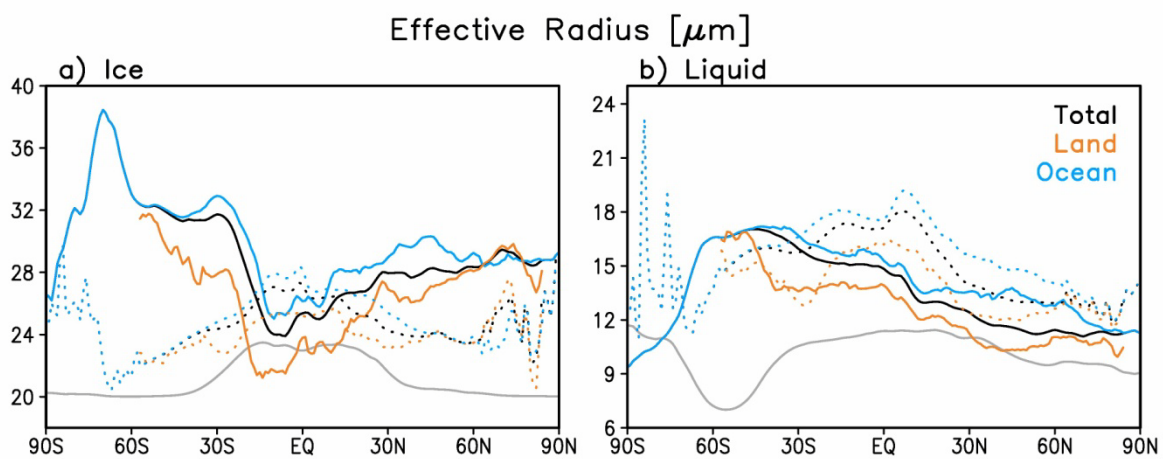


Figure 8

Figure 8. Zonal Average plots of a) ice and b) liquid cloud particle effective radius (μm). Different colors are used for Land, Ocean, and Total (colors legends are displayed in the Plots) for MODIS data (dotted), MAC simulations data (solid), and CTL simulations (gray) (note only one line for the prescribed value for CTL).

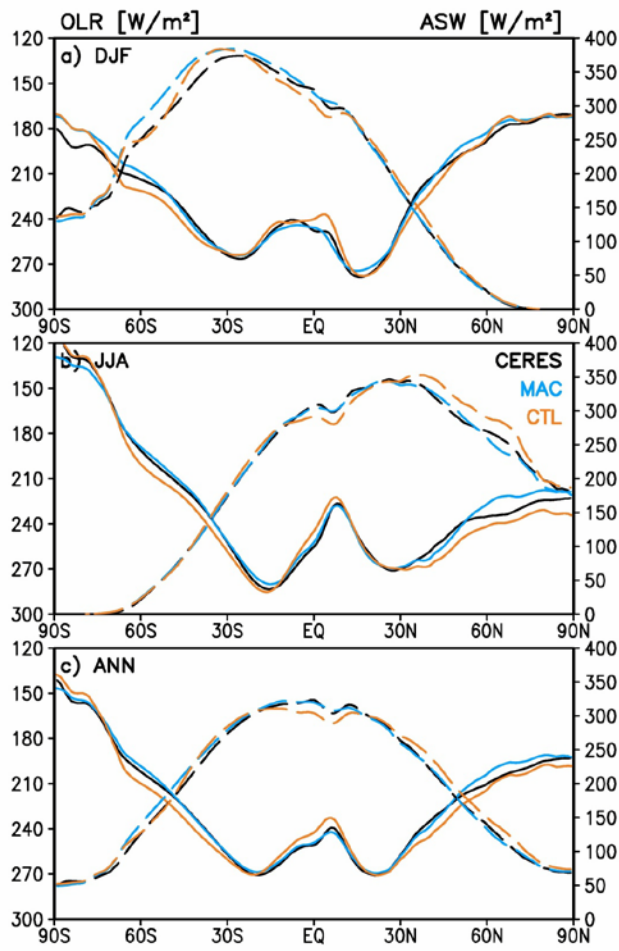
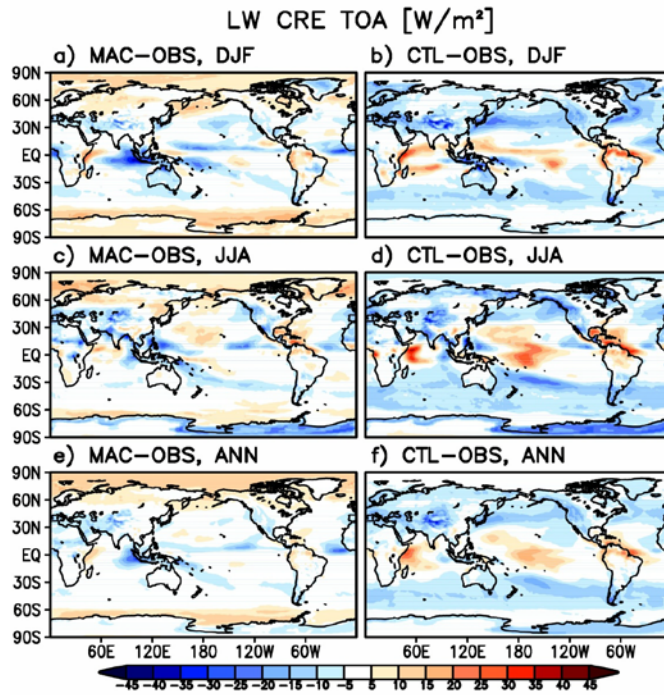


Figure 9

Figure 9.: Zonal average TOA OLR and TOA ASW in Wm^{-2} for DJF (top), JJA (middle), and ANN (bottom). The line colors used for MAC, CTL, OBS are shown in the middle panel.

1

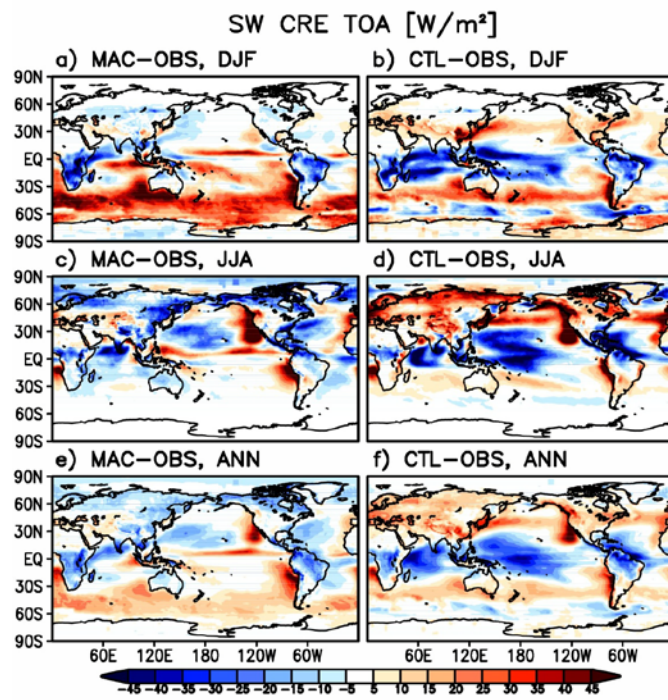


2

3 Figure 10

4 Figure 10.: Distribution of simulated OLR minus OBS CRE TOA in Wm^{-2} . The rows have
 5 DJF (top), JJA(middle) and ANN (bottom). Right (left) columns are for CTL (MAC) data.

6

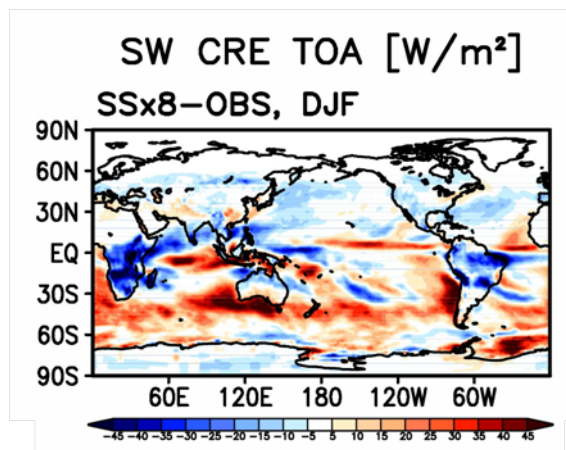


1

2 Figure 11

3 Figure 11.: Same as Figure 10, but for SWA CRE TOA in Wm^{-2} .

4



1

2 Figure 12

3

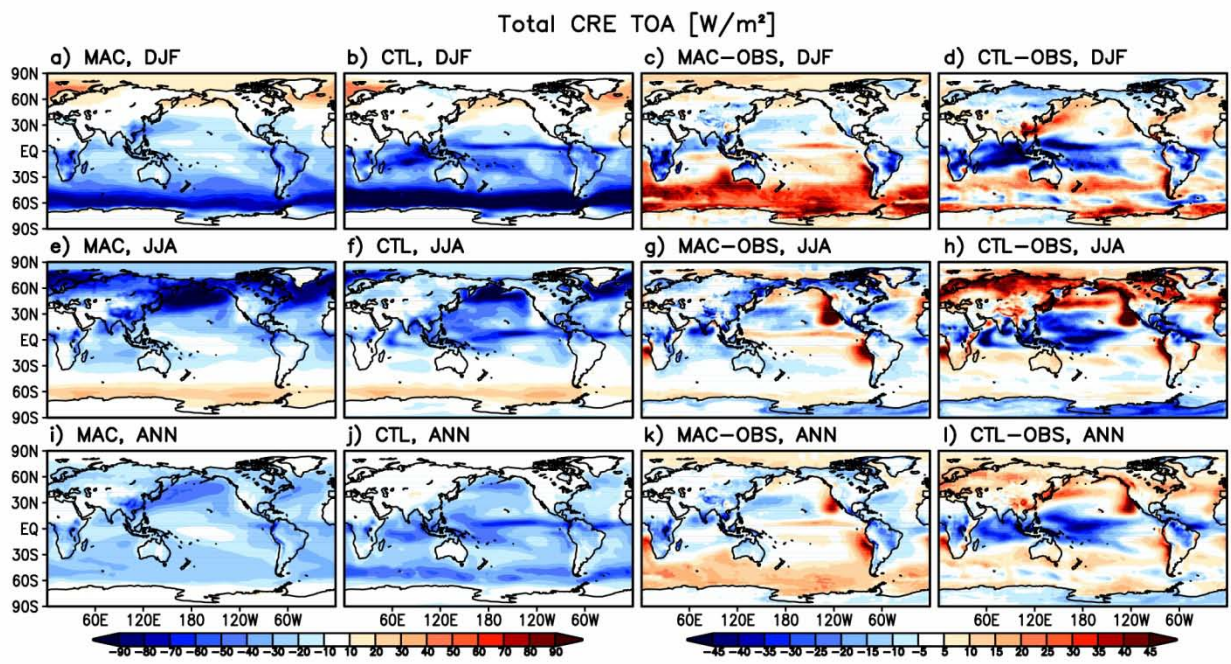


Figure 13